Adaption of 3D Scanning Technology for High Precision Bridge Inspection

Prepared by:
Alexandra Hain, PhD, PE and Arash E. Zaghi, PhD, PE, SE

Report Number:
CT-2310-F-23-2

Final Report

3/31/2023

Research Project: SPR2310

University of Connecticut
School of Engineering
Department of Civil and Environmental Engineering

Submitted to:
Connecticut Department of Transportation
Bureau of Policy and Planning
Research Section

David C. Elder
Transportation Assistant Planning Director

TECHNICAL REPORT DOCUMENTATION PAGE

1. Report No. CT-2310-F-23-2	2. Government Accession No.	3. Recipients Catalog No.
4. Title and Subtitle Adaption of 3D Scanning Technology for High Precision Bridge Inspection		5. Report Date March 31, 2023
		6. Performing Organization Code
7. Author(s) Alexandra Hain, PhD, PE and Arash E. Zaghi, PhD, PE, SE		8. Performing Organization Report No.
9. Performing Organization Name and Address University of Connecticut 261 Glenbrook Rd, Unit 3037 Storrs, CT 06269		10. Work Unit No. (TRIS)
		11. Contract or Grant No. SPR-2310
		13. Type of Report and Period Covered Final Report 02/01/2018 - 06/30/2020
12. Sponsoring Agency Name and Address Connecticut Department of Transportation 2800 Berlin Turnpike P. O. Box 317546 Newington, CT 06131-7546		14. Sponsoring Agency Code SPR-2310

15. Supplementary Notes
A study conducted in cooperation with the U.S. Department of Transportation and Federal Highway Administration

16. Abstract

Corrosion at beam ends is one of the most widespread causes of damage in steel bridges. Accurate determination of the level of section loss due to corrosion damage is critical for estimating the bearing capacity and load rating of a bridge. Current evaluation methods are labor intensive and dependent on subjective assessments by inspectors. Unique features of handheld 3D scanning technology offer significant potential for application in bridge inspections and corrosion damage assessment. 3D scanners can provide accurate information on the pattern and amount of section loss at beam ends. This study evaluated the application of commercially available 3D scanning technology for bridge inspection. The study included both laboratory and field evaluations to determine if the technology could create accurate, high-resolution 3D representations of locally corroded steel beams. The 3D models were used to extract information such as the maximum reduction in thickness and the pattern of corrosion. Additionally, this research project aims to develop a reliable and repeatable protocol for using 3D scanners in bridge inspections. The protocol will include recommendations for scanner settings, data collection and data processing. The project aims to provide recommendations for the integration of 3D scanning technology into bridge inspection programs. The resulting protocol and recommendations will improve the accuracy and efficiency of bridge inspections, reduce the risk of catastrophic failures, and extend the service life of steel bridges.

17. Key Words 3D scanning, bridge inspection, corrosion	18. Distribution Statement No restrictions. This document is available to the public through the National Technical Information Service, Springfield, VA. 22161		
19. Security Classif. (Of this report) Unclassified	20. Security Classif.(Of this page) Unclassified	21. No. of Pages 60	22. Price N/A

DISCLAIMER

The contents of this report reflect the views of the authors, who are responsible for the facts and accuracy of the data presented herein. The contents do not reflect the official views or policies of the State or the Federal Highway Administration. This report does not constitute a standard, specification or regulation.

ACKNOWLEDGEMENTS

The authors wish to acknowledge the support of personnel from the Federal Highway Administration, Connecticut Department of Transportation, and the University of Connecticut. From CTDOT, the authors thank our technical champions Armin Kamali, PE and Robert P. Zaffetti, PE (retired) as well as our support from CTDOT research Bradley Overturf and Flavia E. Pereira, PhD in getting the project off the ground. The authors would like to thank Edgardo Block, Andrew Mroczkowski, and Dionysia Oliveira from the CTDOT Research Unit for their support during the project. The guidance and advice of members of the Bridge Safety and Evaluation Unit of CTDOT is also appreciated. The contribution of Timothy Henning and Ryan Enos in processing the data is acknowledged. The student support of Caitlin O'Brien, Ryan Enos, and Jenette Phillips is also noted.

METRIC CONVERSION FACTORS

APPROXIMATE CONVERSIONS TO SI UNITS				
SYMBOL	**WHEN YOU KNOW**	**MULTIPLY BY**	**TO FIND**	**SYMBOL**
LENGTH				
in	inches	25.4	millimeters	mm
ft	feet	0.305	meters	m
yd	yards	0.914	meters	m
mi	miles	1.61	kilometers	km
AREA				
in^2	square inches	645.2	square millimeters	mm^2
ft^2	square feet	0.093	square meters	m^2
yd^2	square yard	0.836	square meters	m^2
ac	acres	0.405	hectares	ha
mi^2	square miles	2.59	square kilometers	km^2
VOLUME				
fl oz	fluid ounces	29.57	milliliters	mL
gal	gallons	3.785	liters	L
ft^3	cubic feet	0.028	cubic meters	m^3
yd^3	cubic yards	0.765	cubic meters	m^3
NOTE: volumes greater than 1000 L shall be shown in m^3				
MASS				
oz	ounces	28.35	grams	g
lb	pounds	0.454	kilograms	kg
T	short tons (2000 lb)	0.907	megagrams (or "metric ton")	Mg (or "t")
TEMPERATURE (exact degrees)				
°F	Fahrenheit	5 (F-32)/9 or (F-32)/1.8	Celsius	°C
ILLUMINATION				
fc	foot-candles	10.76	lux	lx
fl	foot-Lamberts	3.426	candela/m^2	cd/m^2
FORCE and PRESSURE or STRESS				
lbf	poundforce	4.45	newtons	N
lbf/in^2	poundforce per square inch	6.89	kilopascals	kPa

Table of Contents

LIST OF FIGURES

LIST OF TABLES

Executive Summary

Corrosion is a widespread cause of damage in steel bridges, leading to reduced bearing capacity and possible structural failures. Current inspection methods rely on biennial visual inspections and manual measurements to assess corrosion damage, which may result in inaccuracies that impact safety assessments and prioritization of repairs. To address this issue, researchers at the University of Connecticut conducted a comprehensive two-stage feasibility study, supported by the Connecticut Department of Transportation, to evaluate the potential of handheld 3D scanning and photogrammetry for assessing section loss in corroded steel beams more accurately and efficiently.

The study involved laboratory evaluations of corroded beam sections and field evaluations of in-service bridges, using the advanced Artec Eva and Artec Leo 3D scanners, as well as a Sony a7RIII camera for photogrammetry. The 3D scanning technology demonstrated the ability to provide accurate measurements of corroded regions, offering several advantages for bridge inspections, such as reduced on-site inspection time, improved measurement accuracy, elimination of the need for different measurement tools, and the ability to track deterioration progression over time by overlaying 3D models generated from scans taken at different times.

The use of photogrammetry as a cost-effective alternative to 3D scanning showed promising results but requires further research to explore the accuracy, reliability, and ease of use for section loss assessment in steel beams. Future research opportunities include comparing various camera models and settings for photogrammetry to better understand their capabilities, generating finite element models using scanned geometry to estimate the capacity of corrosion-damaged elements, and proposing simplified design formulations for load ratings to streamline the assessment process. Additionally, research should focus on overcoming challenges such as maintaining object tracking at sharp edges and ensuring proper surface preparation for accurate scanning.

Overall, the study's findings support the use of 3D scanning as a valuable tool for engineers to generate accurate inspection data on corroded regions of bridge beams, improving the safety assessment of bridges and enabling the effective allocation of retrofit funds. The adoption of this technology has the potential to enhance current inspection practices, leading to safer and more efficient management of bridge infrastructure.

1. Introduction and Background

Corrosion is one of the most widespread causes of damage in steel bridges. Corrosion of bridge beams is commonly found directly beneath deck expansion joints, due to leakage of water, deicing chemicals, and contaminants (Figure 1) (1). In some cases, bridges are unnecessarily restricted to traffic, closed, or replaced due to an inaccurate assessment of load-carrying capacity (2). Bearing capacity is reduced by corrosion of the web and bearing stiffeners. The extent of capacity reduction is dependent on the severity of section loss (1, 3). When localized bearing forces are combined with areas of extensive section loss, failures such as web crippling can occur (Figure 1b). The bearing capacity and load rating of a steel beam is directly dependent on the degree of section loss. Therefore, it is critical that the geometry and the extent of section loss are accurately assessed by inspectors.

Figure 1. Corrosion at beam end resulting in (a) a hole in the bearing stiffener (Photo Courtesy of Luis Vila) and, (b) web crippling (Photo Courtesy of Michael Culmo).

Currently, a biennial visual inspection is the basic starting point to evaluate the condition of a bridge (4). Section loss measurements for corrosion damage are performed using measuring tools such as tape measures, rulers, calipers, and in some cases, Non-Destructive Testing (NDT) such as ultrasonic thickness gauges. These measurements are limited to the overall height and length of the corroded area as well as the maximum section loss in that area. The accuracy of on-site measurements is dependent on if the inspector has correctly identified the extent of the corroded area. Any inaccuracies in field measurements may lead to misguiding condition assessments (5). Because the inspection outcomes have a substantial impact on the safety assessment of bridges and prioritization of repairs, there exists a critical need for objective techniques that provide accurate information on the geometry of corrosion damage (6, 7). This information enables engineers to reliably assess the remaining load-carrying capacity of corrosion-damaged beams.

High-resolution 3D scanning has the potential to address this shortcoming by enhancing the precision of the underlying measurements used in bridge inspections. Currently, the use of 3D scanning in civil engineering has been limited to large-scale models to represent the as-built or existing geometry of a structure (8-10). Terrestrial laser imaging, such as light detection and ranging (LiDAR), is a method of data acquisition that may be used to create 3D point clouds for bridge structures (11-15). Various laser scanners are available with a typical range of accuracy between 3–

50 mm when placed at a distance of 100 m (0.12-1.97 in at 328 ft) (16). However, this level of accuracy is not sufficient for capturing local geometric information such as that of corrosion damaged regions. The assessment of corrosion damage may require sub-millimeter point accuracy.

Structured-light 3D scanning technology enables sub-millimeter point accuracy (17). This method of scanning has been used in other fields, such as mechanical engineering, archeology, medicine, and criminology (18-20). The principle of structured-light imaging is to extract the 3D surface shape based on information from the distortion of a projected structured-light pattern (21). The scanner projects a series of reference patterns onto the surface of an object, collects the distorted pattern with cameras, and uses algorithms to calculate surface information (21). This information can be represented as a point cloud, surface mesh, or solid model. In addition to collecting detailed geometric information, structured-light scanning is unique in its ability to capture the color and texture of an object. This data may be used to generate 3D renderings to supplement the photographs and sketches used in inspection reports as shown in Figure 2. Such features of structured-light scanners make the technology attractive for the corrosion damage assessment of bridges. In addition to obtaining accurate geometric information, this technology may offer several other advantages for use in bridge inspections including: 1) reducing the time required by inspectors on-site, 2) eliminating the need for different measurement tools, 3) evaluating the progression of deterioration by overlaying 3D models generated from scans taken at different times, 4) providing detailed measurements at multiple locations, 5) enabling the verification of measurements following an inspection, and 6) improving measurements by thoroughly cleaning the beam end to remove deleterious corroded and laminated steel.

Figure 2. Sample of 3D model of corroded bridge beam generated with 3D scanning.

3D scanning is rapidly emerging as a reliable and effective technique for capturing precise measurements and creating models to track the progress of corrosion. Prior studies have demonstrated the significant improvement in the assessment of section loss caused by corrosion

through the use of this method 3 (22). However, to provide reliable and accurate data for corrosion damage assessment, high levels of precision are essential. While commercially available scanners can provide sub-millimeter point accuracies, the cost of these devices may be prohibitive. For instance, the scanner utilized in the study on section loss assessment had an impressive point accuracy of 0.1mm and retailed for $19,800 (23). Photogrammetry presents a promising alternative to 3D scanning for achieving similar modeling results at a significantly lower cost. This technique involves creating a 3D model of a subject using the analysis of two-dimensional photographs (24). The process is based on calculating coordinates from multiple images of an object taken from different angles (25). The more pictures used, the more reference points can be created, increasing the accuracy of the 3D coordinates of the object. Photogrammetry has been previously demonstrated as a viable imaging technique in civil engineering applications (26). Aerial photogrammetry is commonly used by state Departments of Transportation for applications such as topographical mapping as well as mapping of transportation systems and construction sites (26). Photogrammetry has recently been used for capturing movements and measurements on smaller scales in several research studies. This includes the structural analysis of a masonry bridge in Spain (27), measuring the imperfections in cold-formed steel members (28), and as a method for corrosion assessment of steel reinforcing bars (29). While photogrammetry is not a new concept, recent advances in camera resolution and computer processing power have made it a more viable technique, reducing the time required to generate a model. Photogrammetry offers several advantages, including significant cost reduction and maneuverability. However, the accuracy and ease of use of photogrammetry for section loss assessment of steel beams have not been fully explored for this application.

To evaluate the potential of handheld 3D scanning and photogrammetry for the section loss assessment of corroded steel beams, a two-stage feasibility study was conducted by researchers at the University of Connecticut (UCONN) as part of a study supported by the Connecticut Department of Transportation (CTDOT). The first stage of the research consisted of a laboratory evaluation in which corroded beam sections were scanned at UCONN. The second stage consisted of six field evaluations in which corroded beam ends were scanned on in-service bridges in Connecticut (Figure 3). The suitability of the scanning technology for corrosion assessment was based on the ability to accurately capture the geometry, color, and texture of the sections in both environments. The scanning data from both stages was used to generate 3D models, which were found to be detailed digital replications of the physical objects. Thickness measurements from the 3D models were compared with measurements taken by other instruments. The accuracy of the measurements indicates that 3D scanning technology has the potential to improve the quality of bridge inspection data while simplifying the on-site data collection process.

Figure 3. UConn research team and CTDOT on site for field scan with Artec Eva.

This report provides an overview of different scanning technologies and equipment as well as results, general observations, and conclusions drawn from the laboratory and field trials. It is anticipated that the conclusions and observations presented will provide support for the use of 3D scanning as a tool for engineers to generate accurate inspection data on corroded regions of bridge beams. This data may be used to inform decisions regarding load postings, prioritization of rehabilitation projects, and the allocation of retrofit funds.

2. Research Approach

The research approach section of the report will provide a detailed description of the equipment and techniques used for both handheld 3D scanning and photogrammetry. This section will cover the selection criteria for the scanners, their specifications, and the software used for data processing. Additionally, the section will elaborate on the data collection process, including the procedures for capturing and processing the images and scans. The report will also discuss the data processing techniques employed to extract measurements, such as corrosion area and section loss, from the 3D models generated by both techniques. Overall, the research approach section will provide a comprehensive overview of the methods and techniques used to carry out the study and will offer insights into the challenges and limitations of each technique.

For more information on the 3D scanning process with the Artec Leo, please see **Appendix A – Video Tutorials for 3D Scanning for Corrosion Damage Assessment of Steel Beams**. These videos provide an overview of the scanning process from unboxing the Leo to processing field data. For more information on a related using photogrammetry for the evaluation of dry stone masonry retaining walls, please see **Appendix B – Case Study on Photogrammetry for Dry Stone Masonry Retaining Wall Inspection.**

2.1. Overview of Scanning Technology

2.1.1. Handheld 3D Scanning Equipment

To evaluate the applicability of 3D scanning for use in the assessment of section loss due to corrosion, it was first necessary to find a commercially available scanner well-suited to the application. After a review of the accuracy, size, and portability of several commercially available scanners, the Artec Eva scanner, shown in Figure 4a, was chosen. The scanner retails for $19,800. The 0.85 kg (2.2 lb) 3D scanner is a handheld unit that requires an external power source and a computer. For both the on-site and laboratory trials, a laptop and battery pack were used to provide mobility. The selected scanner has an accuracy up to 0.1 mm (0.004 in), a resolution up to 0.5 mm (0.020), a working distance of 0.4 to 1 m (1.31 to 3.28 ft), and a linear field of view of 214 × 148 mm to 536 × 371 mm (8.43 × 5.83 in to 21.1 × 14.6 in). The scanner has a video frame rate of up to 16 frames per second, an exposure time of 0.0002 seconds, and a data acquisition speed of up to 2 million points per second (17). Additionally, the scanner does not require calibration as the scanner is pre-calibrated prior to delivery. However, the calibration of the scanner should be checked periodically to ensure the measurements are reliable. The calibration can be checked by scanning an object of known dimensions, such as a ruler, and comparing the measurements from the scanner with the known values.

In this study, a gaming laptop (i7-7700HQ CPU at 2.8 GHz, 32 GB RAM, and NVIDIA GTX 1070, 8 GB

GDDR5 GPU) was used to run the scanner to ensure that computing power would not be a limiting factor (Figure 4b). The laptop retails for $2,100. This computer exceeds the minimum requirements for the scanner including an Intel i5 or i7 processor, 16 GB of RAM, and a video card with 1 GB of video memory (17). The necessary computing requirements are further evaluated in the discussion section of this paper. Artec Studio 11 software, which was included with the purchase of the scanner, was used for operating the scanner and processing the data.

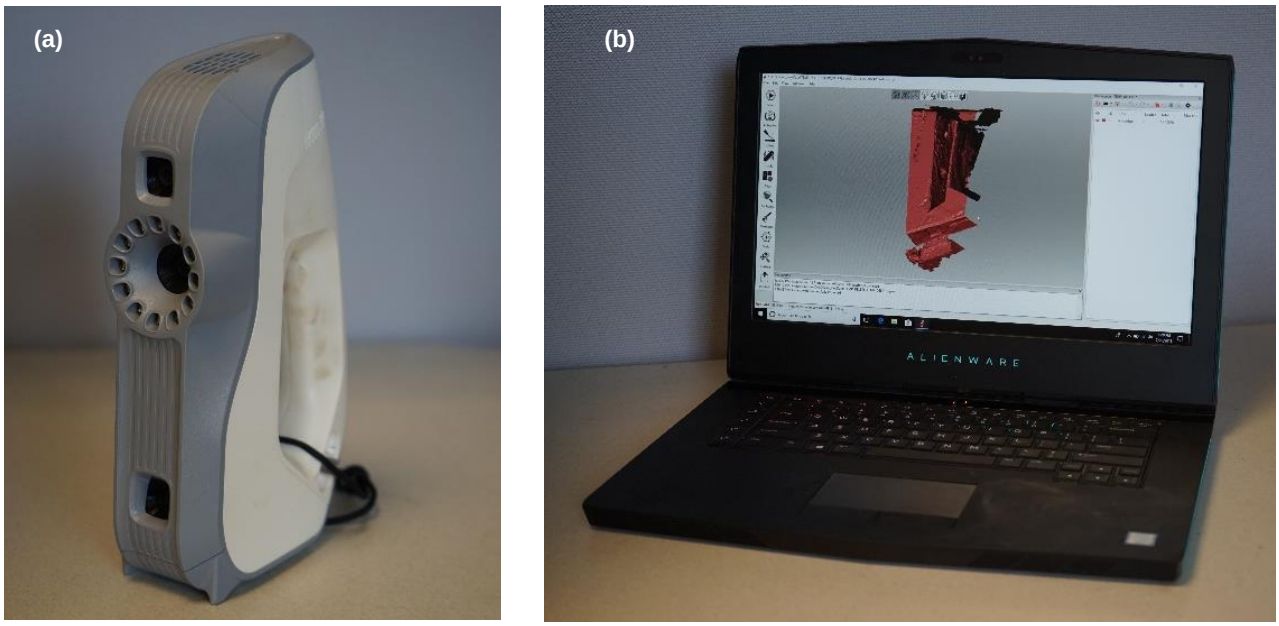

Figure 4. Equipment required for scanning including the (a) Artec Eva scanner and (b) Alienware laptop.

It is crucial for professionals in any field to keep up with technological advancements to stay competitive and relevant. In the field of structural engineering, the application of new technologies, such as 3D scanning and photogrammetry, can significantly improve the accuracy and efficiency of bridge inspections and corrosion damage assessment. As demonstrated in the study, the use of handheld 3D scanning technology in bridge inspections provides a more objective and detailed assessment of corrosion damage. Near the end of the study, the 3D scanner was switched from the Artec Eva to the Artec Leo, which offers several key benefits. The Artec Leo, shown below in Figure 5, features an integrated touch screen and onboard processor, enabling real-time data processing and reducing the need for a separate computer. The device also includes a built-in battery, making it more mobile and eliminating the need for a power source. The Leo's advanced tracking algorithms and high-resolution color cameras provide even greater accuracy and detail, making it an ideal tool for bridge inspections and corrosion damage assessment. Overall, staying up-to-date with technological advancements is essential for professionals to ensure they are utilizing the most effective tools and techniques to achieve the best results.

Figure 5. Updated 3D scanning equipment the Artec Leo shown a) in carrying case and b) in field.

2.1.2. Photogrammetry

To evaluate the applicability of using photogrammetry, it was first necessary to find commercially available equipment to capture pictures and a computer with a powerful graphics processing unit (GPU) to process the data. While a standalone GPU is not required for photogrammetry, it substantially increases the speed of processing. A powerful GPU is required by the software that was chosen in this study. The most critical pieces of equipment are the camera and lens used to capture images. Photogrammetry relies on the ability to detect features in an image. Higher-resolution cameras allow the sensor to resolve small features from further distances. For this reason, the Sony a7RIII with a 42-megapixel 35-mm full-frame sensor was selected (30). The lens chosen was the low-distortion Zeiss Batis 2/25 with a focal length of 25 mm, an aperture range of f/2 to f/22, and a minimum focusing range of 0.2 m (8 in) (31). This wide-angle lens has a large field of view, which decreases the number of images required while providing the large overlap between images that are needed for future image processing. Using a low-distortion lens limits the distortion compensation required in data processing and significantly improves the quality of raw data. Distortion happens when the image scale is not constant throughout the entire image field and causes straight lines to bend inward or outwards from the center of the image. In addition to the camera and lens, a powerful flash was needed to provide even lighting and mitigate slight variations in natural light. To alleviate the differences in lighting onsite, a Godox flash (32) was used. The camera, lens, and flash are shown in Figure 6. .

In this study, a desktop computer was used to run the software that processed the images and generated the 3D model (AMD Ryzen Threadripper 2990WX CPU at 3.0 GHz, 128 GB RAM, and ZOTAC GeForce GTX 1080 Ti 22GB GDDR5X GPU). This computer was chosen to increase the processing speed. The software, RealityCapture, was used to generate the 3D model and will be discussed in the data processing section of the report.

Figure 6. Equipment used for photogrammetry including the camera, lens and flash.

2.2. Data Collection

2.2.1. Handheld 3D Scanning Equipment

The Artec Eva and Artec Leo scanners are handheld structured-light scanners. Structured-light scanning works by projecting a series of patterns onto the object, usually in the form of multiple parallel beams. When the patterns are projected onto the surface of the object, they become distorted. By measuring the deformation of these patterns, the scanner can calculate coordinate points to generate a point cloud. The scanner captures these images and the corresponding software uses triangulation to calculate the depth of the object and surface texture to create a 3D model (21, 33). The device's two high-resolution color cameras then capture the patterns as they are reflected back from the object, creating a detailed 3D image. Because the distance between the scanner and each point on the object's surface is known, the resulting 3D model is automatically to scale. The automatic scaling feature of structured light scanning is one of the key advantages of this technology over photogrammetry.

During the scanning process, the laptop (for the Eva) or the scanner itself (Leo) provides a real-time image of the data being collected as shown in Figure 7. This allows the user to ensure that the bridge geometry of interest has been scanned. When scanning a homogenous surface, targets should be placed on the object to provide tracking points as the scanner is moved. To collect data, the user passes the scanner in a side-to-side motion from the top to the bottom of the object keeping the scanner relatively perpendicular to the surface of interest. The scanner may be rotated to capture all areas of interest, but rotating the scanner at extreme angles may cause issues with tracking. If there are issues with tracking, the scan will be terminated and a new scan file will be generated. At the conclusion of scanning, the geometry and texture of the object is pre-processed and saved. This is the most time-consuming step and is greatly influenced by the processing speed of the computer used.

Figure 7. Representative view showing beam section scanned with Artec Leo in the field. Areas shown in red detail where information is missing.

The use of alignment bars is crucial for handheld 3D scanning when it is not possible to close the loop. Closing the loop refers to the process of scanning a full 360-degree view of an object and connecting the start and end of the scan. When this cannot be achieved, alignment bars become an essential tool to ensure accurate and consistent results.

Alignment bars provide a known reference geometry that the scanner can use to align and stitch together multiple scans. By incorporating these bars into the scanning process, the scanner can more accurately determine the position and orientation of the scanned object in 3D space. This helps to reduce the accumulation of errors that may occur during the alignment process, ultimately resulting in a more precise 3D model. Furthermore, alignment bars can be particularly useful in situations where complex geometries or tight spaces make it difficult to capture the entirety of an object in a single scan. Utilizing alignment bars in such scenarios can greatly improve the overall quality and accuracy of the final 3D model, ensuring reliable data for subsequent analysis and structural assessments. Different alignment bars and tracking tools are shown below in Figure 8.

Figure 8. Representative views showing different tracking markers used for handheld scanning.

2.2.2. Photogrammetry

The accuracy, quality, and completeness of the 3D model generated from photogrammetry is dependent on serval factors. Photogrammetry works by identifying common objects in a series of photographs. This requires overlap between images, pictures taken from different orientations, and complete coverage of the object to generate a comprehensive 3D model. To ensure optimal results in photogrammetry, it is crucial to create an image collection plan prior to capturing images. This plan should specify the distance of the passes, the range of camera shot heights, the distance between images for proper overlap, and any areas of complex geometry that may require additional high-resolution images to ensure full coverage. This plan should be reviewed and modified for each shoot, depending on the available space and equipment used.

In addition, certain steps should be taken before capturing images to achieve the best results in photogrammetry. Shiny and low-textured objects can pose challenges in the alignment process, as reflections from shiny surfaces can change positions depending on the orientation of the camera, and low-textured objects lack identifying marks to match up between pictures. To address these issues, shiny surfaces can be dulled down with dulling spray or powder, while low-textured surfaces can be marked up with a writing implement or tape (see Figure 9 below). Reference markers should also be placed near the object to aid the software in image alignment and scaling the model during post-processing. After prepping the area, images can be captured according to the collection plan.

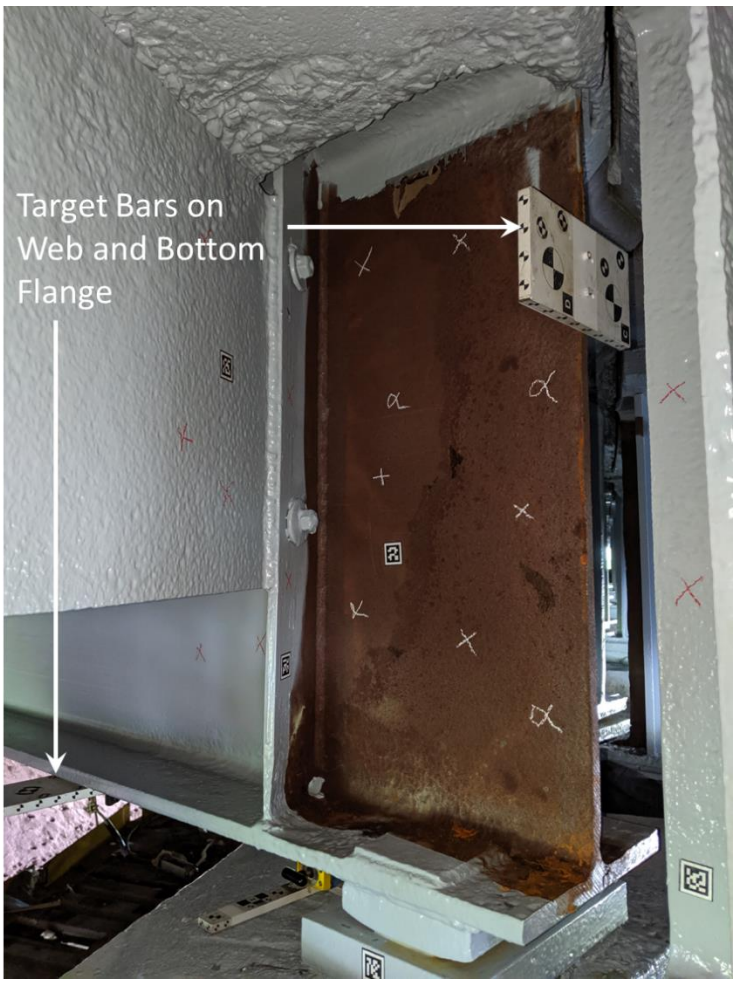

Figure 9. Representative view showing web and flange tracking bars used for handheld scanning.

For structures such as beam ends, it is critical to capture images from a distance to provide a baseline reference scene as well as close-range pictures to increase the accuracy of the model. Sets of images taken at different offset distances will be referred to as passes. To ensure the software is capable of matching features between the “far-pass” and “near-pass” images, linking passes should be added. Through data-collection trials, it was found that the distance between passes should be less than two times the distance of the previous pass. The distance of the first pass should be based on the target accuracy as well as the resolution of the camera. Similarly, the overlap of images is important within a given pass.

For the software to generate depth maps and the 3D coordinate system, images of the object are needed from different perspectives. This requires multiple images of each feature at different horizontal and vertical orientations (Figure 10). This can be accomplished by moving the camera from the left to right and tilting it to collect images from every angle. Both the number of passes as well as the number of images with different orientations should be increased for areas of concern that require additional detail.

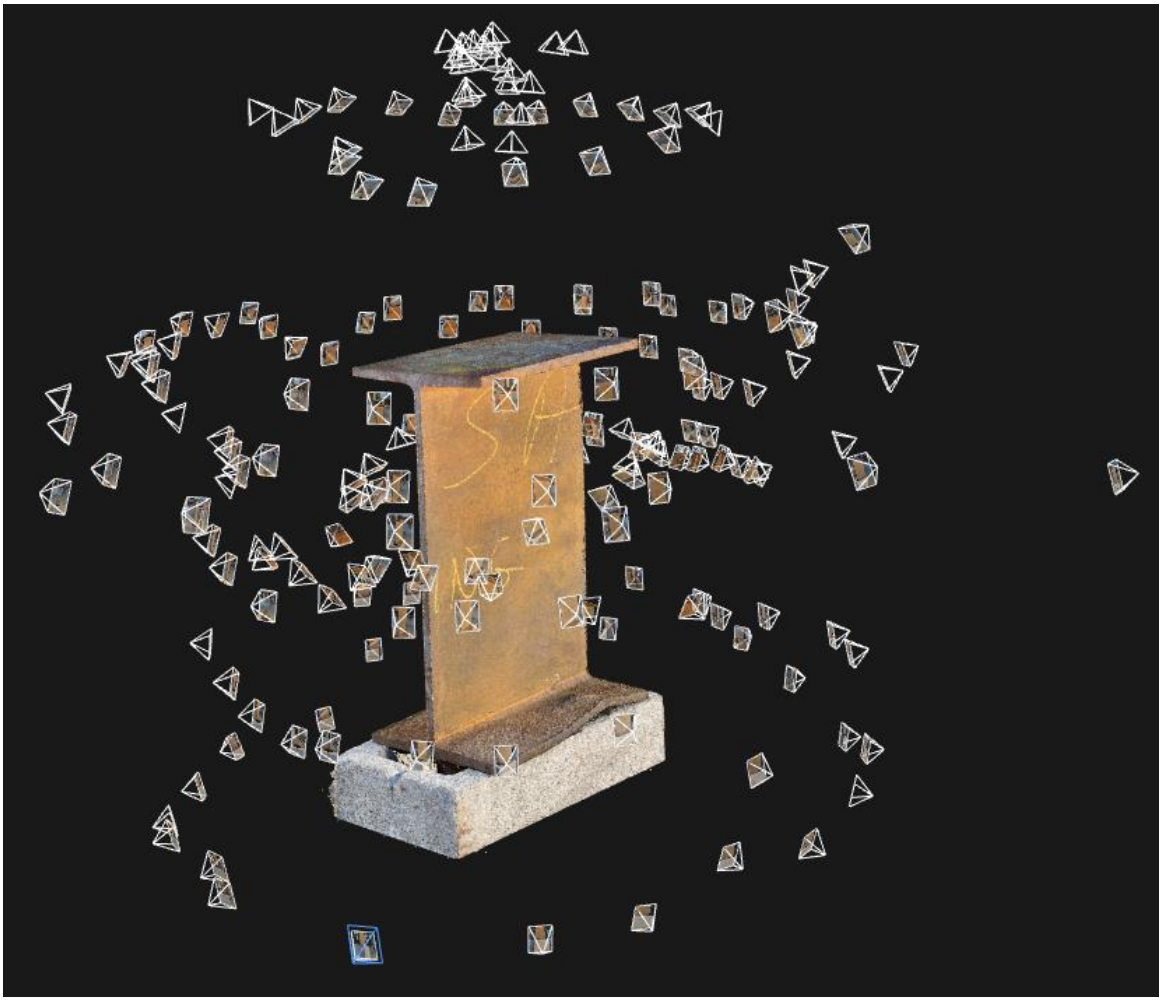

Figure 10. Representative view of 3D model generated with photogrammetry showing location and orientation of photos.

Photogrammetry requires user input to correctly represent the scale of a scene. This can be accomplished by measuring an object within the scene and using it as a reference, such as the height of the beam or thickness of the bottom flange, or by including scale markers. For high-accuracy applications, using scale markers is preferred as they provide known measurements rather than estimations. Scale markers should be easy to identify within images, contain references with known dimensions, and be placed on a rigid backing to prevent distortion of the scale marker. In this trial two types of markers, grid and cross-type, were printed and affixed to thick glass or fiberglass backings. The markers are shown in Figure 11. In the software, these markers are used to define distance relationships.

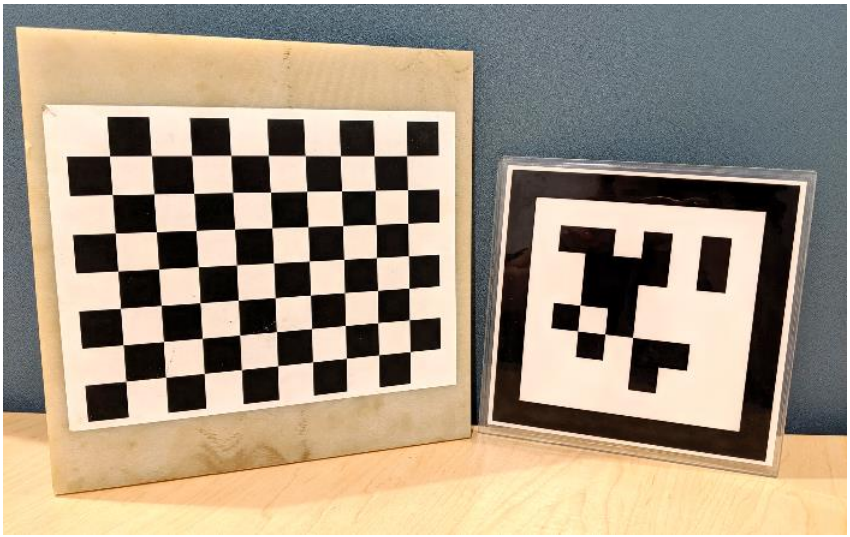

Figure 11. Sample reference markers used for photogrammetry.

2.3. Data Processing

2.3.1. Handheld 3D Scanning

All post-processing of scanning data takes place in the office. Data post-processing includes erasing excess scan data, aligning individual scans, and merging the scans. All post-processing was completed in the manufacturer's software. The first step in post-processing is deleting extraneous data points to reduce the size of the overall data set. Extraneous points were removed by manually selecting and deleting areas such as the pier cap, underside of the deck, and the abutting beam. After the manual deletion of points, an outlier removal algorithm was applied in the software to remove noise. The outlier removal uses a statistical algorithm that calculates the mean distance between every surface point and a certain number of neighboring points, as well as the standard deviation of these distances. The points that have mean distances higher than a range defined by the global distances mean and standard deviation are then removed.

The second step involves aligning individual scans. Scans are aligned using common geometric and/or textural references. Scans on the same face of a beam can be aligned automatically as the software can recognize overlapping geometric and textural references. Scans on opposite or adjacent faces can be aligned manually by identifying at least three points in common on two overlapping scans. This process is repeated as needed to align all individual scans. As such, the complexity of post-processing is reduced by using fewer scans. However, a sufficient number of scans must be collected to capture all required geometric information otherwise the model fidelity may be compromised. Additionally, there must be an overlap in the scan files being combined for alignment purposes. As access to bridge beams is limited, more data than is required should be collected. Once the data is collected, the most comprehensive scans can be selected to reduce the overall number of scans required for post-processing. Once the scans are aligned, they are merged into one set of surface data. At this point, the model only contains point cloud and geometric surface data. The texture and color information from select scans can then be applied to the newly created surface. Merging of scans and mapping of textures are time-consuming operations, but once the command is selected no further input is required from the technician. The speed of the operations is dependent on the processing power of the computer used. The final model includes the point cloud and the merged surface model with texture. A sample view of the interface for data

processing in Artec Studio is shown below in Figure 12.

Figure 12. Sample view of data-processing interface in Artec Studio.

2.3.2. Photogrammetry

All processing of the images takes place offsite. Prior to processing, all images that are not relevant, out of focus, or not correctly exposed should be removed from the batch. After the initial sorting is complete, the images are imported to RealityCapture in JPG format. RealityCapture is a commercially available all-in-one photogrammetry software that automatically extracts 3D models from images (34). This software is unique in its speed, ability to produce high-polygon meshes, and built-in editing and mesh simplification features.

After importing, the images need to be aligned. This is done by first performing a draft alignment and then adding control points to the image. Control points should be identified in multiple images from different viewpoints. The points are manually added to help the software link images or components together that it is having difficulty joining automatically. The points are also used to add reference measurements to the scene. Once the distance constraints are applied, the model is updated and realigned. An alignment report for the model is generated that notes the projection error, which is the difference in pixel position between a point in a photo and the projection of the corresponding 3D point in the same photo. Ideally, the median error should be around 0.5 pixels, and not above 1 pixel. If the error is above this threshold, additional control points are added manually to the model by selecting common features in multiple images and the alignment process is run again. This process is repeated until the target accuracy is achieved. A longer measurement relative to the alignment markers can also be used as a check for the generated model.

After alignment, the final step in processing is to generate a mesh. This is the most time-consuming operation, and the speed is dependent on the complexity of the model, the resolution and number of images used, and the processing power of the computer. To decrease the processing time, non-critical areas can be left out of the defined “Reconstruction Region”. The final mesh can then be used for measurements or be exported to additional software to obtain additional information or

visualizations. A sample view of the interface for data processing in RealityCapture is shown below in Figure 13.

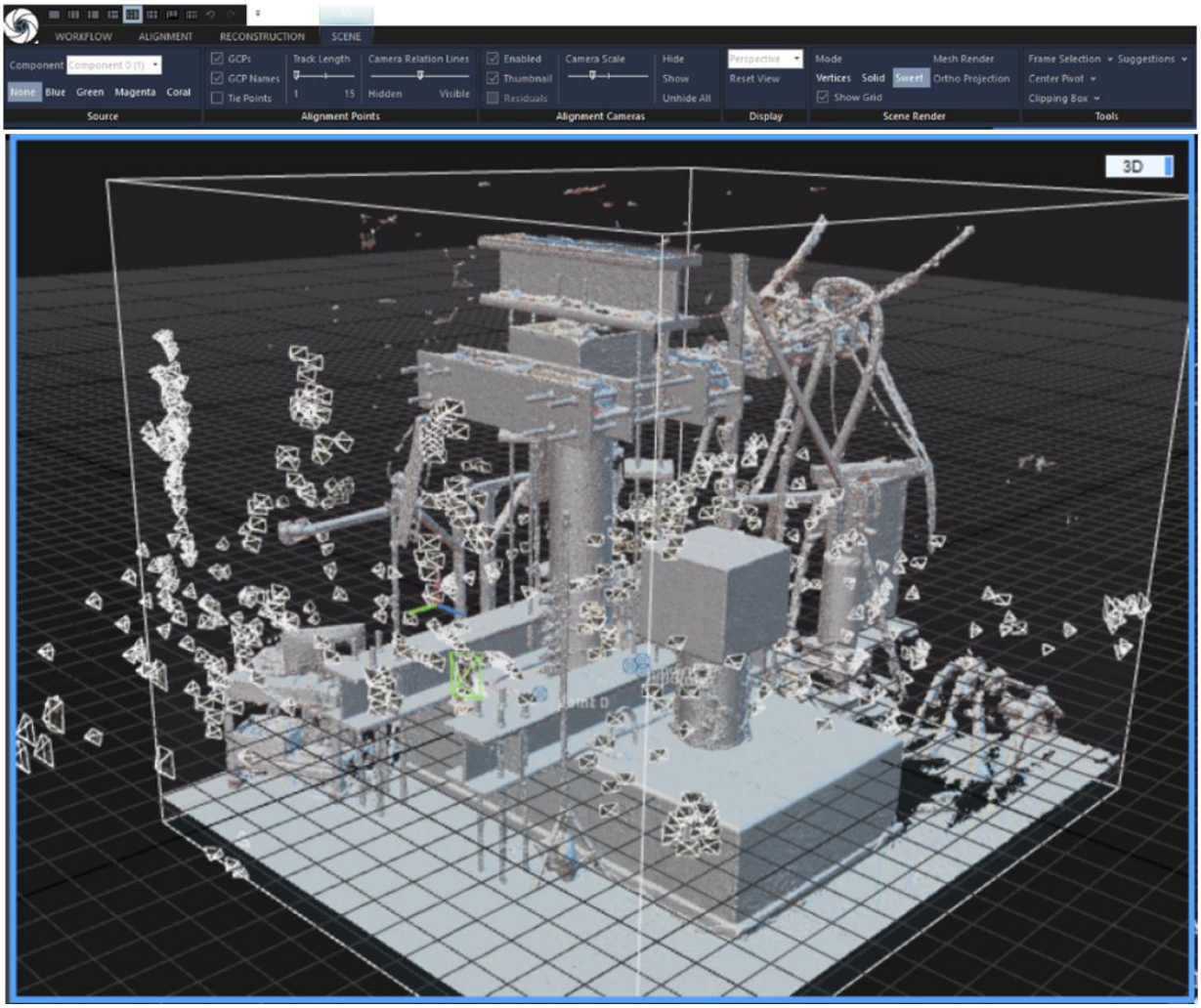

Figure 13. Sample view of data-processing interface in RealityCapture.

3. Findings and Applications from Laboratory Trials

3.1. Handheld 3D Scanning

The success of the laboratory trial was based on three criteria: the ease of use of the scanner, the quality of the 3D representation of the specimen produced by the scanner, and a comparison of thickness measurements obtained with the scanner and with an ultrasonic thickness gauge. For the first criterion, using the scanner was straightforward. Its lightweight and the clip-on battery pack provided mobility.

The second criterion was evaluated by comparing the 3D model with a photograph of the beam. Both images are shown below in Figure 14. The 3D model (Figure 14b) has small crosshairs on the surface to assist with tracking for the scanner. These trackers were applied after the initial picture (Figure 14c) was taken. The 3D model was able to reproduce the color and pattern of the corroded section. The similarity between the images shows the capability of the scanner to capture both the geometry and color of the overall specimen.

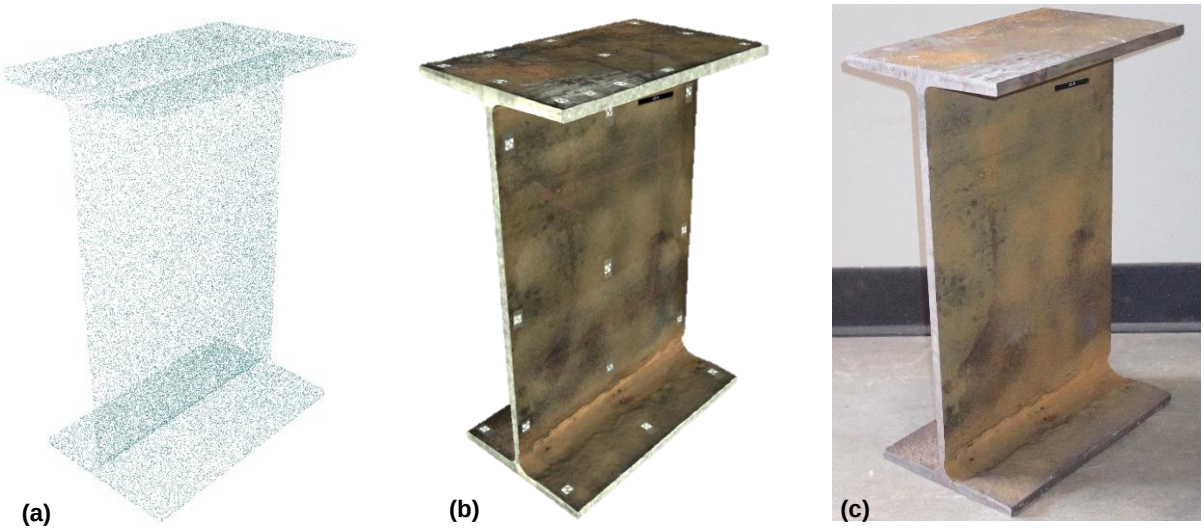

Figure 14. Visual of section from laboratory trial: (a) point cloud, (b) 3D scan with texture, (c) picture of section.

The third criterion was evaluated by taking thickness measurements in the manufacturer's post-processing software and comparing them with those obtained with an ultrasonic thickness gauge. Comparisons between thickness measurements were limited to the intact portions of the web as surface roughness and sharp gradients can adversely affect the accuracy of the thickness probe. The maximum deviation in measurements between scan data and the gauge was 0.1 mm (0.004 in). Thickness measurements in the software were taken on the web of the beam in both the corroded and intact regions. A sample thickness measurement (in millimeters) taken in the post-processing software is shown below in Figure 15a. The software also allows users to take section cuts along any plane. A sample section cut is shown in Figure 15b. The cut plane is shown in blue, and all areas where the beam and the plane intersect are outlined in green. This tool automatically calculates the perimeter and area of the section outlined in green, as well as the volume on either side of the cut. This allows engineers to see and understand the profile of section loss due to corrosion at different locations.

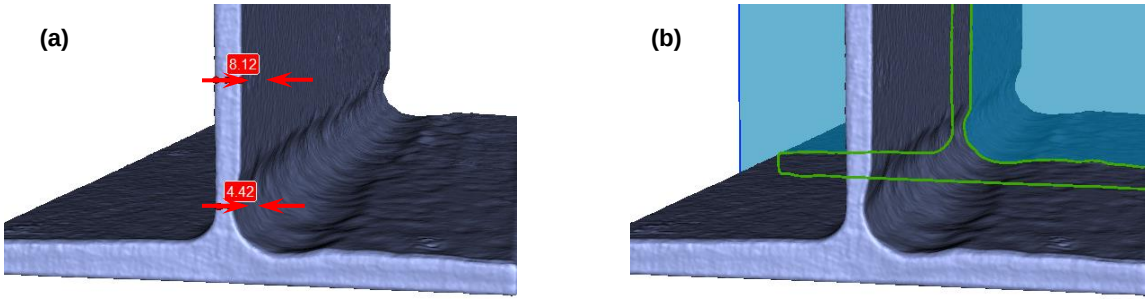

Figure 15. Measurements taken with the post-processing software including (a) linear measurements in mm and (b) a section cut.

In addition to the immediate benefits of improved section loss measurements, 3D scanning also offers opportunities for enhanced tracking of bridge deterioration. Overlaying 3D models from scans taken at different times allows for visualizing the progression of corrosion. This is demonstrated below in Figure 16. The beam shown in green is the same corroded section shown

in Figure 14 and Figure 15. This beam was highlighted green to show a clear distinction between the two surfaces. The intact section, shown in brown, was an intact section salvaged from an equivalent beam. Overlaying scans from different times allows engineers to visualize the rate of deterioration to help anticipate future rehabilitation needs.

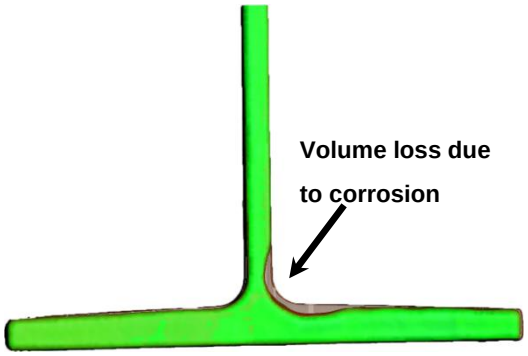

Figure 16. Visual representation of intact section overlaid with corroded section in the post-processing software.

An outdoor trial was necessary after completing the indoor scanning to account for different temperatures and lighting conditions that replicate field conditions. Scanning in controlled indoor environments typically does not provide accurate representations of objects in the field. Outdoor conditions may include different weather conditions, lighting, and varying distances between objects, which can impact the accuracy of the scans. Conducting outdoor scans ensures that the technology and techniques used in the study are reliable and effective in real-world scenarios. This trial provides valuable insights into the potential limitations and challenges of using handheld 3D scanning technology and photogrammetry in field conditions and helps to establish best practices for future fieldwork. During scanning, the laptop shows a real-time image of the data being collected. This allows the operator to ensure that the geometry of interest is being collected. Individual scans are generated during the scanning process when the individual file sizes get large, tracking of the scanner is lost, or the user generates a new scan. In this study, data collection consisted of 3 overlapping scans that were generated over a period of approximately 30 minutes. A view of scanning the girder specimen prior to testing is shown in Figure 17. At the conclusion of scanning, the geometry and texture of the object are pre-processed and saved.

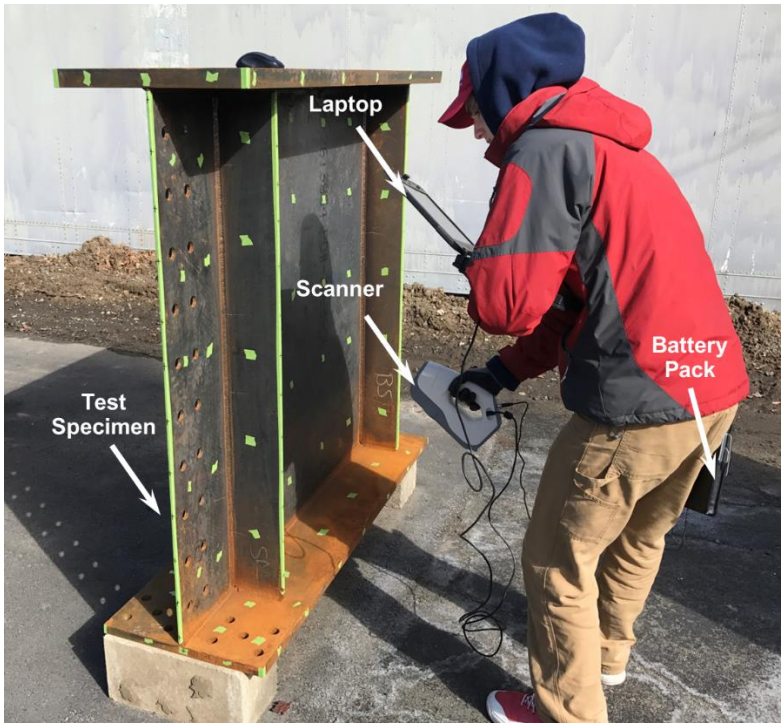

Figure 17. Scanning of beam end with simulated corrosion damage.

Data processing using the software provided by the scanner manufacturer is required to convert the scan data collected into the 3D model. This includes erasing excess scan data, aligning the individual scan sets, and merging the scans. The first step in processing is to manually delete extraneous data points from other objects captured during scanning, such as the ground in this trial. This reduces the size of the overall data set, which reduces the computation time for processing. After the manual deletion of points, an automated outlier removal algorithm was run to reduce the noise in the data.

The second step in processing is aligning individual scans. Scans are aligned using common geometric and textural references, including the markers applied to the scanning surface. Scans can be aligned automatically if the software recognizes overlapping references or can be aligned manually by identifying at least three points in common on two overlapping scans. This process is repeated as needed to align all individual scans.

Once the scans are aligned, they are merged into one set of surface data that includes both the point cloud and surface mesh. The texture and color information can then be applied. Merging scans and texture mapping is computationally demanding. For the trial, processing took approximately 2 hours. The final 3D mesh of the beam was limited to the full height of the bearing column. This region was selected to reduce model size while capturing the corroded region. The model represented an area of approximately 1 m^2 and consisted of approximately 70 million vertices. The final data set, including the point cloud, merged surface model, and texture model, was approximately 2 GB in size. A close-up view of the 3D model showing the front and side view of the corroded region of the girder end is shown in Figure 18a and b, respectively.

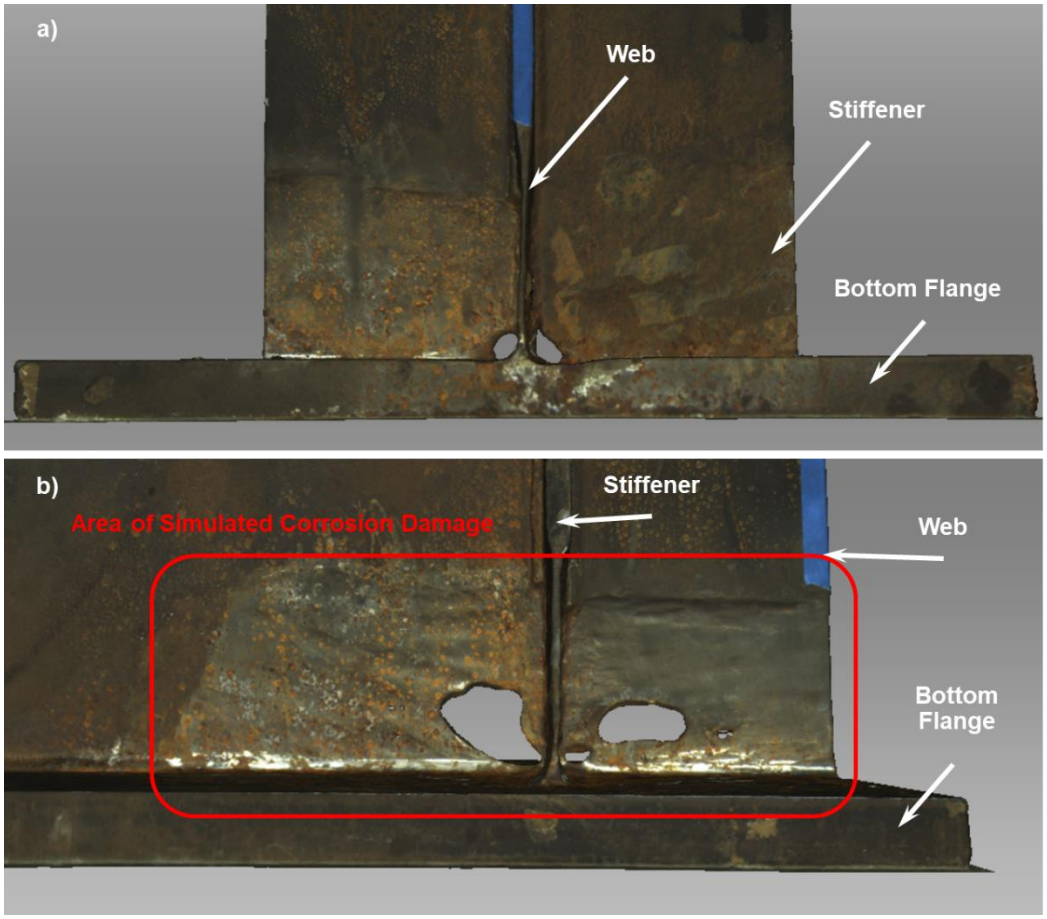

Figure 18. Close up of corroded region on the 3D model generated from the scan of girder showing a) front view and b) side view.

3.1. Photogrammetry

A beam of similar size and condition to the one scanned in the first field trial for the handheld scanner was selected for the photogrammetry trial. The same beam was no longer available as the photogrammetry trial was conducted over a year after the scanning trial. Prior to imaging, lighting adjustments were made to enhance image quality. This was achieved by using floodlights on either side of the beam, ensuring that all parts were well-lit and clearly visible. The selected specimen was neither shiny nor smooth, which eliminated the need for additional markings or dulling. The beam's width was measured from corner to corner for later use in scaling the model. In the four trials, images were collected as shown in Figure 19. The images were captured laterally, encircling the beam at a close range to obtain the appropriate number of images for each trial. These close-up images primarily contributed to determining the model's texture. Additional images were taken from a greater distance to guarantee thorough coverage of the beam. Following data acquisition, images were uploaded to RealityCapture, where they were sorted, aligned, scaled, and processed into 3D models.

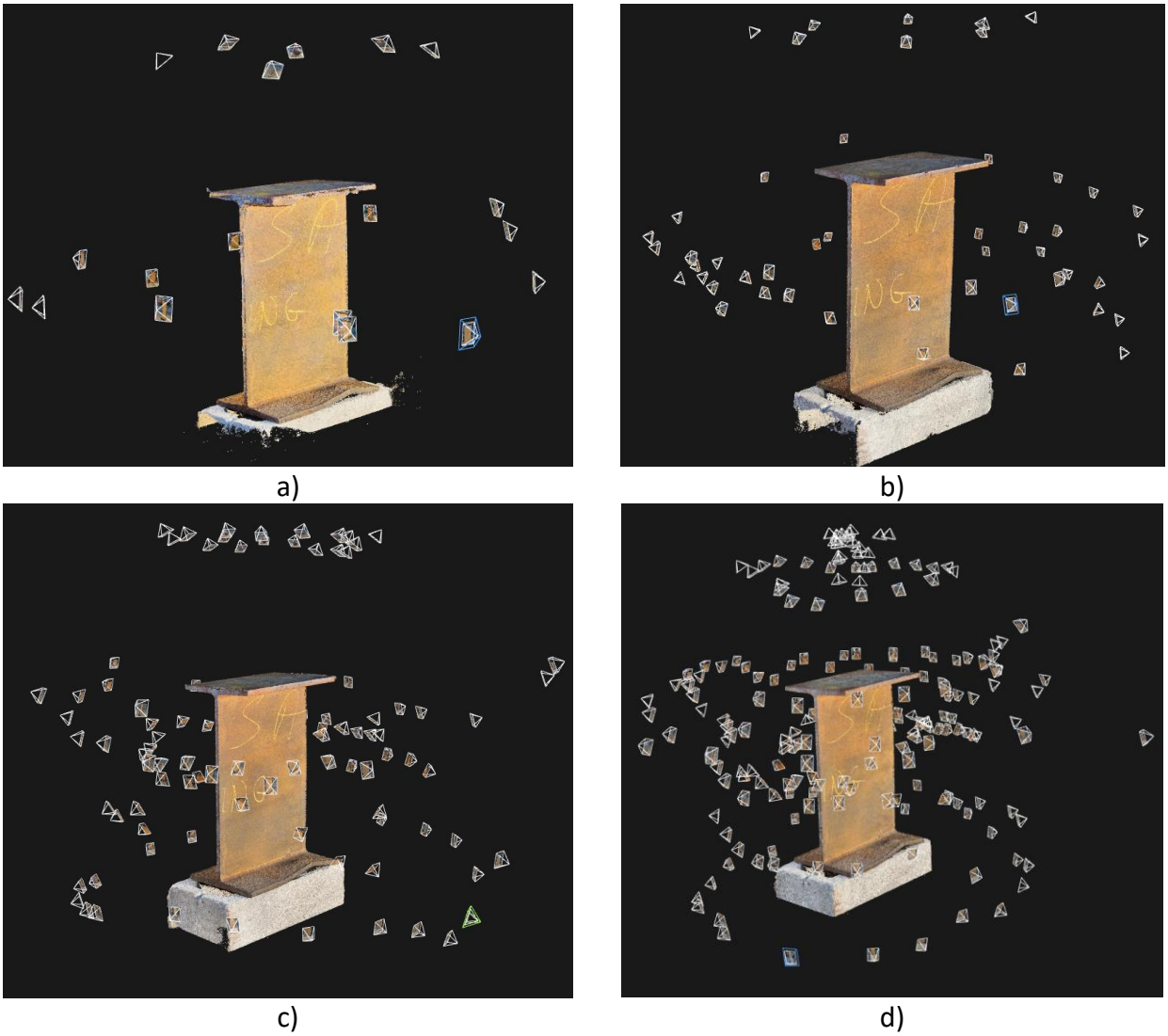

Figure 19. Imaging locations for each laboratory trial including a) 20, b) 50, c) 100, and d) 200 image trials.

The models generated using the Sony a7RIII are displayed below in Figure 20. Upon visually examining the quality of the generated models, it was evident that the Sony models followed the suspected trend - a higher number of images resulted in a better-quality model. The higher number of photos allowed for a more accurate reconstruction of the object by providing additional reference points and better coverage of the object's surface. This increased accuracy led to a high-quality 3D model that closely resembled the actual object and provided more reliable measurements for further analysis.

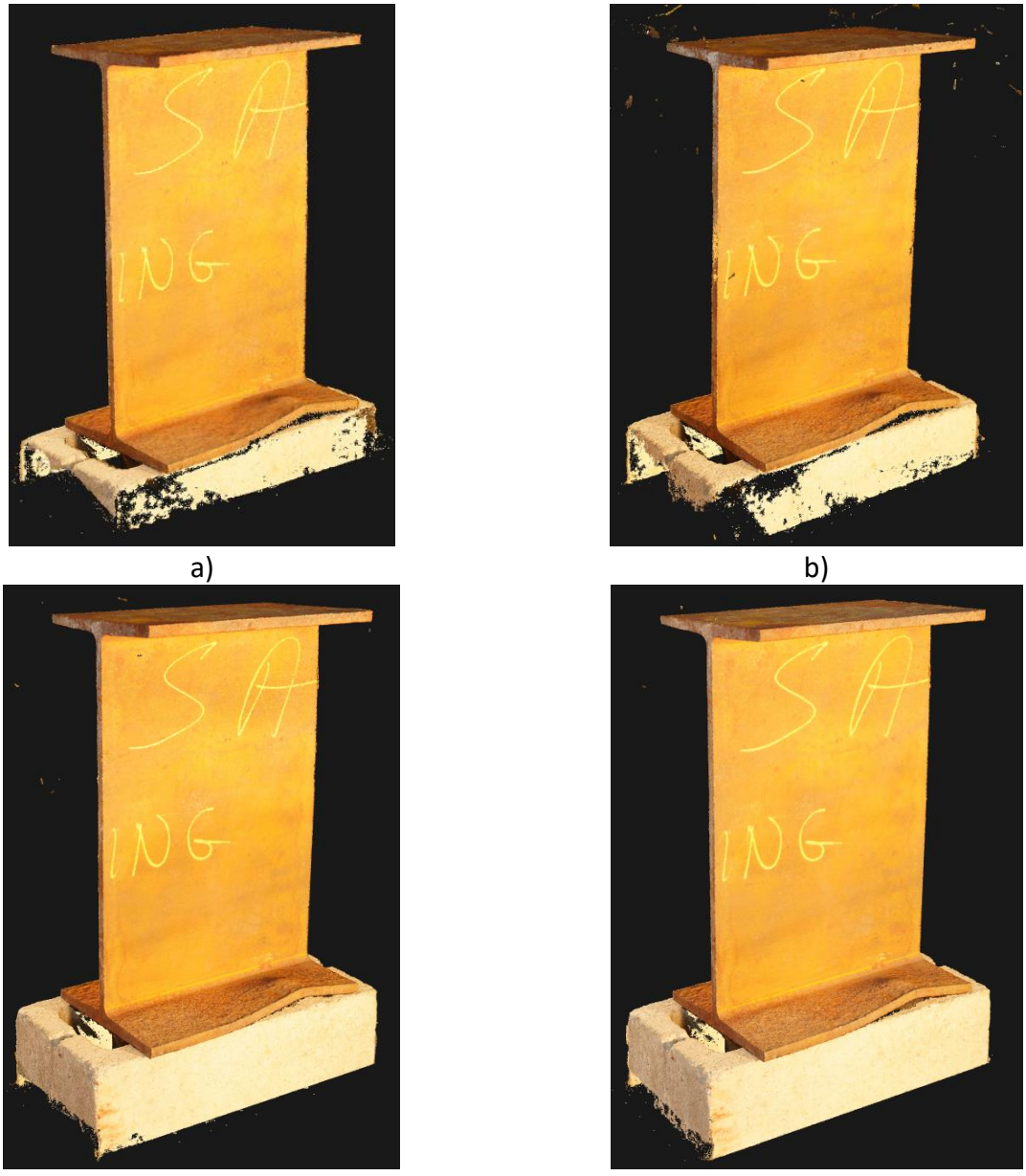

Figure 20. Lab trial photogrammetric reconstructions created with a) 20, b) 50, c) 100, and d) 200 Sony a7RIII images.

For the 20-image models, RealityCapture could only create them after adding numerous control points and running the alignment several times. This process was extremely time-consuming and could have been avoided by simply capturing more images. The 50-image models were more manageable but still required many manual alignments and took several hours to complete. On the other hand, the 100 and 200-image trials were much easier to model, as they required minimal manual processing. The 100-image trials took about 45 minutes to complete, while the 200-image trial took around an hour.

In addition to a visual comparison, the 200-image trials were compared to a baseline scan using the Artec Leo at locations specified in Figure 21. The 200-image trial was selected because the model generated with this number of images was the most accurate. The measurements are given and compared to the baseline laser scan in

Table 1.

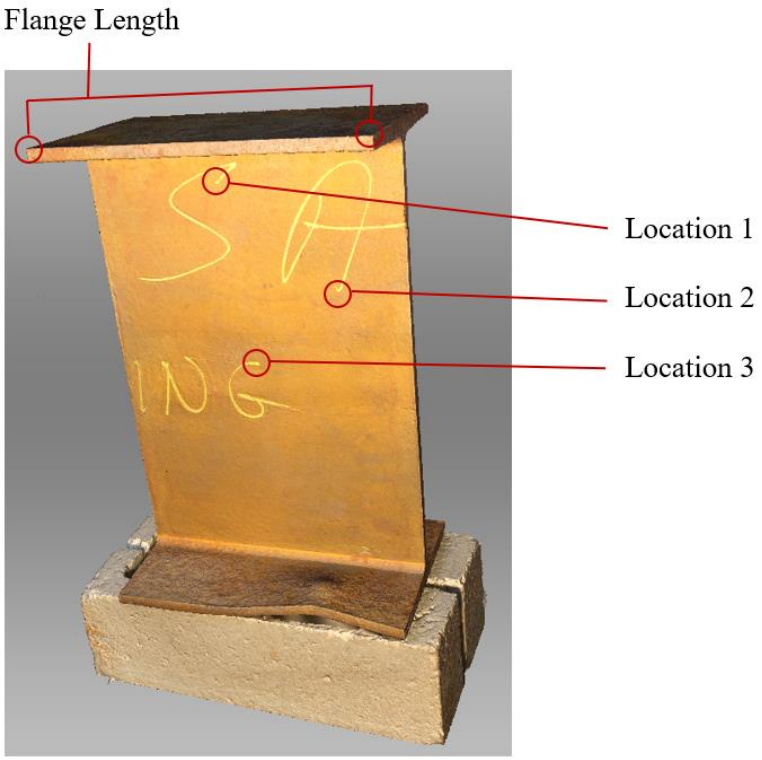

Figure 21. Lab trial measurement locations.

Table 1: Thickness measurements at various locations on the lab beam

Imaging Device	Flange Length (mm)	Flange Length Percent Error	Thickness at Location 1 (mm)	Thickness at Location 2 (mm)	Thickness at Location 3 (mm)	Average Thickness Percent Error
Artec Leo	303.40	0.069%	9.3	9.7	9.7	----------
Sony a7RIII	303.60	0.003%	8.7	9.4	9.4	4.5%

The table presents a comparison between the Artec Leo and Sony a7RIII imaging devices in terms of the measurements obtained for flange length and thickness at various locations. The percent error for each measurement is provided, which helps in evaluating the accuracy of the devices compared to a baseline manual measurement for flange length and between the devices for web thickness measurements.

For flange length, both devices show very low percent errors compared to the baseline manual measurement, with the Sony a7RIII having a slightly lower error (0.003%) compared to the Artec Leo (0.069%). This indicates that both devices are capable of providing accurate measurements for flange length.

When comparing the thickness measurements at three different locations, the Sony a7RIII exhibits an average thickness percent error of 4.5% relative to the baseline Artec Leo measurements. This suggests that the Sony device offers a reasonable level of accuracy in capturing the thickness of the object. However, it is important to consider that, at such fine scales, the error could potentially stem

from the Artec Leo itself. Without a manual data point comparison, this analysis can only demonstrate the relative similarities between the two methods and is not sufficient for determining which method performs better. Therefore, further investigation with manual measurements would be beneficial to provide a more comprehensive comparison of the two devices' accuracy in capturing object dimensions.

Based on the provided data, both imaging devices appear to perform well in terms of accuracy for flange length measurements when compared to the baseline manual measurement, able of to provide sub-millimeter accuracies. Overall, both devices demonstrate the potential to provide accurate measurements, making them suitable for capturing object dimensions in the context of corrosion damage assessment and structural engineering applications. Future research is needed to compare the full surfaces of the models rather than only select points.

4. Findings and Applications from Field Trials

4.1. Handheld 3D Scanning

After conducting the laboratory trials, the research team felt confident in their ability to utilize handheld 3D scanning technology and photogrammetry to capture accurate and detailed images of corroded steel beams. The lab trials provided valuable insights into the capabilities and limitations of the technology and allowed the team to develop a comprehensive protocol for data collection and processing. Armed with this knowledge, the research team was ready to move on to field trials to test further the accuracy and effectiveness of the technology in real-world conditions. The field trials were designed to simulate the challenging conditions of bridge inspections, including outdoor environments with varying lighting and weather conditions as well as access constraints. The team was eager to apply their findings from the lab trials to the field and to refine their approach based on the results of the outdoor trials. Overall, the transition from lab trials to field trials represented a significant step forward in the research project, as it allowed the team to move beyond controlled laboratory conditions and begin to explore the real-world applications of handheld 3D scanning technology and photogrammetry in bridge inspections and corrosion damage assessment.

During the field trials, six structures were scanned, showcasing a range of construction dates and materials. These structures included West Hartford (built in 1969), Glastonbury (built in 1959), Colchester (built in 1966), Avon (built in 1950), New Haven (built in 1965), and East Hartford (built in 1987). The trial encompassed both rolled beam bridges and plate girders, as well as plain carbon steel and weathering steel. The report will provide two representative examples to illustrate the scanning process: one where the focus was on scanning only one side of the beam and another where a full 3D representation was created. These examples will help demonstrate the effectiveness of structured light scanning in assessing the integrity of various structures, emphasizing the importance of thorough surface preparation and accurate scanning techniques.

4.1.1. Trial 1

The success of the field evaluation was based on the quality of the 3D representation of the specimen and the ability to safely use the scanner on-site. For the first criterion, values such as the average depth of section loss, the height of corrosion, and length of corrosion were compared to a recent inspection report. While the maximum section loss values were similar, the scan data

showed how the profile of section loss varied. Therefore, the load rating based only on the maximum section loss would be overly conservative. Per discussions with CTDOT, the measurements for the height, length, and depth of the corrosion from the scanner were used as a baseline and compared with those from the inspection report. The fidelity of the scan data is demonstrated by the similarities between the 3D model and photographs of the beam end (Figure 22).

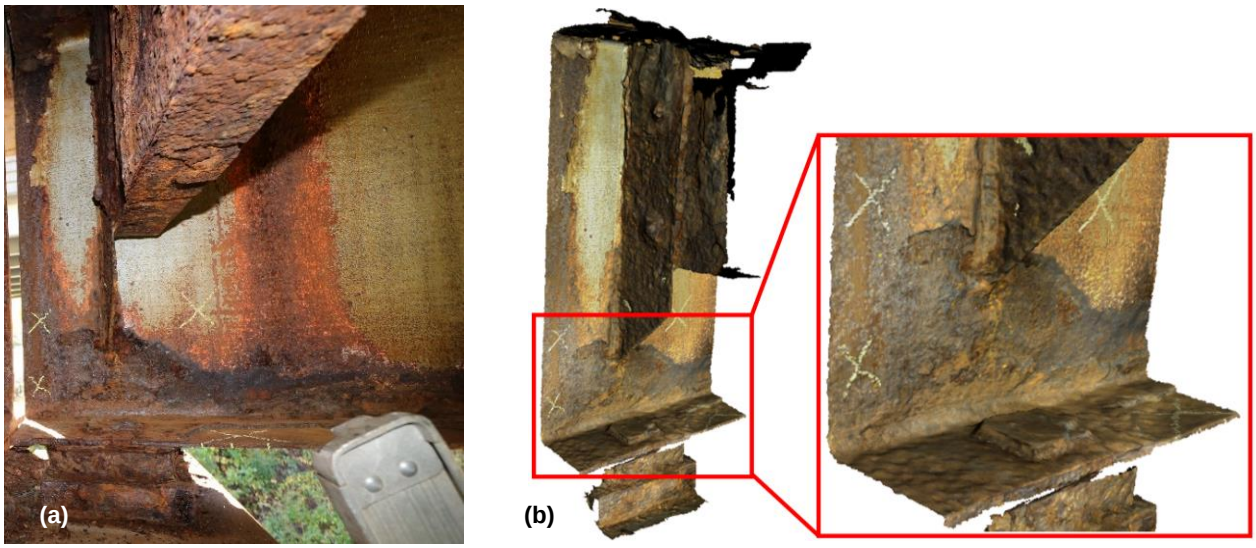

Figure 22. Images from field trial (a) photograph and (b) 3D model.

In addition to viewing the scan data in the manufacturer's software, supplementary tools can be used to provide further clarity of the in-situ geometry of a section. An example is shown in Figure 23 where color mapping is used to highlight the severity of section loss. Figure 23a shows the texture of the beam without color and Figure 23b shows a color map of the difference between a baseline intact surface and the existing surface. In Figure 23b, the differences in color denote the severity of section loss, with red being the most severe. This provides significant insight into the condition of the component and reveals details that are not immediately evident in the typical illustrations and pictures currently used in inspection reports.

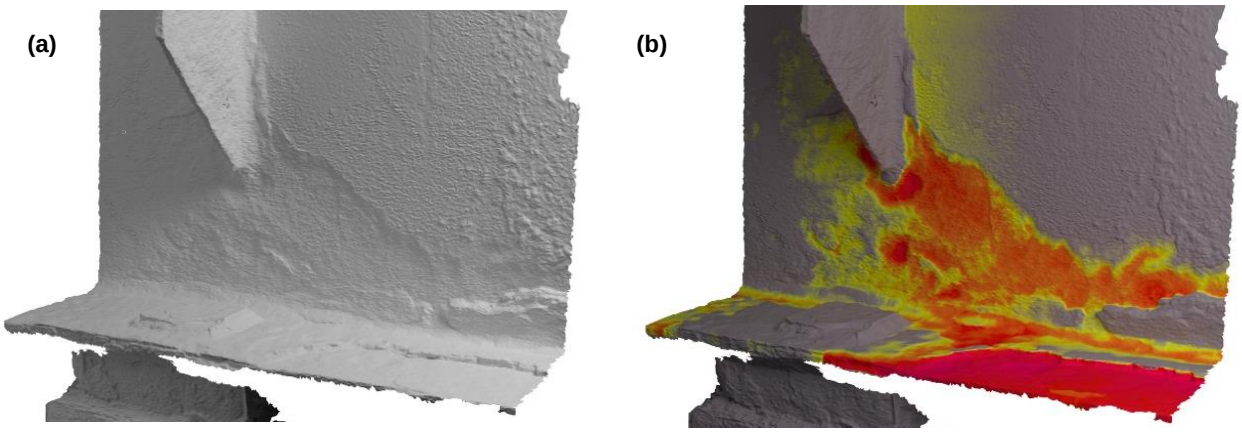

Figure 23. 3D model of beam face showing a) texture and b) coloring mapping to illustrate severity of section loss.

For the second criterion, the scanner was easy to use on-site. The laptop could be placed on the pier cap, allowing for mobility. On bridges where there is not a flat, easily accessible surface for the laptop, use on-site may prove challenging. Additional considerations for the successful application of 3D scanning in field conditions will be noted in the discussion section.

4.1.1. Trial 2

The success of the field evaluation was based on the ability to collect data on both faces of the beam end and align the sides in post-processing to create a complete 3D model. After post-processing, the thicknesses of areas without section loss in the model were checked to ensure the surfaces were plane. The alignment was validated by comparing measurements in the model with known references such as the length and thickness of the reference object. Once the geometry of the model was determined to be representative of field conditions, section loss measurements from the model were compared to the most recent inspection report. Color mapping was used to identify the minimum remaining thickness in the model. Figure 24a shows the model of the beam with color and texture and Figure 24b shows a color map of the remaining thickness. In Figure 24b, the differences in color denote the remaining thickness, with red being the most extreme section loss, or the minimum remaining thickness. At the location of the maximum section loss the remaining thickness noted in the inspection report was 6.35 mm (0.25 in). However, by using the section cut tool in the scanning software, the remaining thickness was approximately zero. This demonstrates how locating the area of the maximum section loss can be facilitated by using the 3D model and supplementary tools.

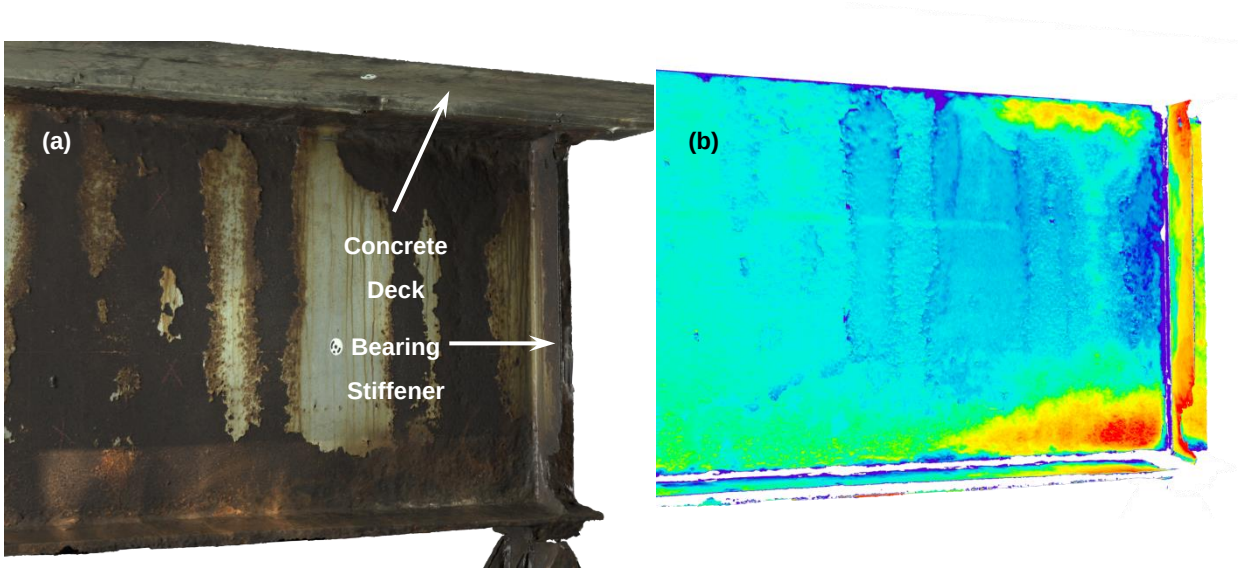

Figure 24. 3D model of beam end showing a) texture and b) coloring mapping to illustrate remaining thickness.

4.2. Photogrammetry

In this study, photogrammetry was utilized to evaluate only one structure, as the main focus was on structured light scanning. The field evaluation was conducted on a bridge in Connecticut, examining a beam end with a skew of approximately 26 degrees. Around 400 images were taken using a Sony a7RIII camera, allowing for the assessment of imaging formats, ease of use, and maneuverability in tight spaces. The beam end was prepared by spraying it with dulling spray and marking it with chalk

to enhance textural features and improve tracking and alignment. Reference markers were placed, and camera settings were adjusted for variable lighting conditions.

Despite the high resolution, the limited space under the bridge made it challenging to capture images from various orientations with the Sony camera, resulting in holes and discontinuities in the 3D model. Both RAW and JPEG formats were tested, with JPEG being selected for this study due to its faster processing time and reduced need for manipulation. The camera flash may have over-illuminated the scene, affecting image quality. More trials are needed to understand the impact of lighting on camera modeling ability, and using flood lighting might yield more accurate models due to uniform lighting.

Future research opportunities include exploring the use of additional markers for improved alignment, as well as investigating the batch processing of RAW images. These advancements could enhance the overall efficiency and accuracy of the photogrammetry process in assessing structural integrity, complementing the structured light scanning techniques employed in this study.

5. Conclusions, Recommendations and Suggested Research

5.1. Recommendations and Suggested Research

The trial applications of the Artec scanners yielded successful results. However, before implementing structured-light scanning for section loss assessment, several factors must be considered. These include scanning corners and sharp edges of objects, scanning shiny surfaces and surfaces with laminar rust, and scanning in direct sunlight. Additionally, potential uses for scanning data beyond geometric measurements are discussed.

Both laboratory and field trials revealed challenges in maintaining object tracking at sharp edges, leading to additional scans and increased post-processing time. Taking multiple passes of edges with the scanner can help capture sufficient data and mitigate this issue. Scanning highly reflective surfaces can also be challenging, as structured-light scanners project light beams onto a surface and measure the deformation of these patterns. Reflectance and ambient light changes may cause inaccuracies. This concern was managed in the laboratory trial by covering the reflective surface with tape or talcum powder. Field-specific considerations include removing laminar rust to ensure a clean surface for comprehensive scanning, as it is essential to thoroughly clear the beam since structured light scanners only capture surface details. Insufficient cleaning can lead to an overestimate of residual thickness, which may result in the inspector not detecting dangerous situations where the structure's capacity is severely impacted. Proper surface preparation is crucial for accurate assessment of the structural integrity of the beam. This is highlighted below in Figure 25 that shows 3D scans taken before and after cleaning of the beam. It is evident that substantial material was removed during cleaning.

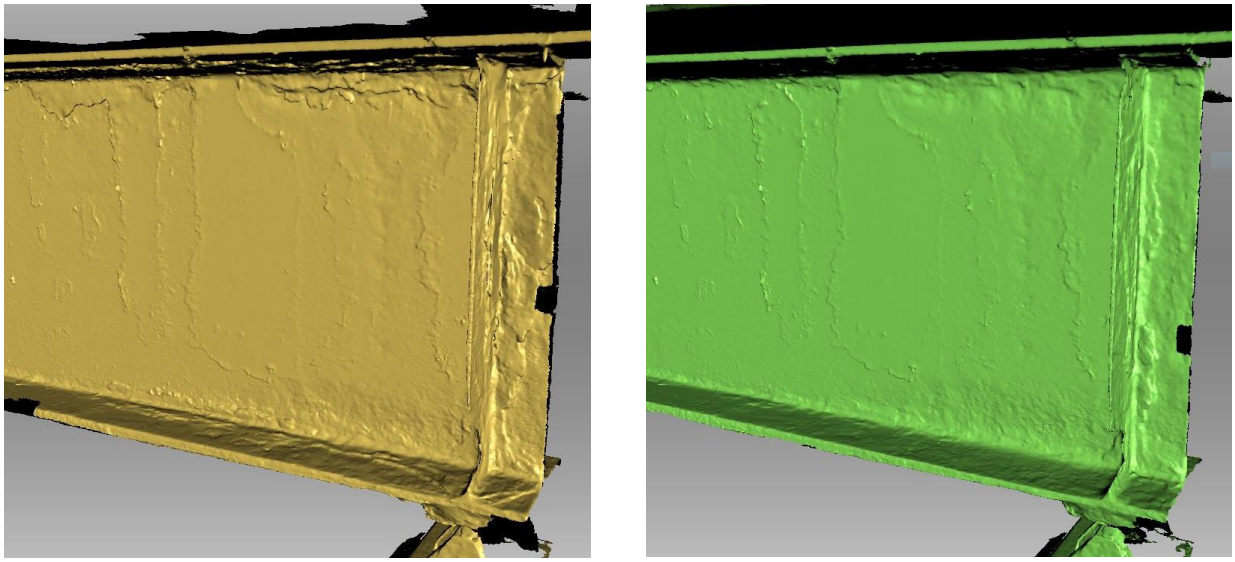

a) b)

Figure 25. Representative image of 3D scans taken a) before cleaning and b) after cleaning.

3D scanning data offers additional benefits beyond geometric measurements. The data produced by structured-light scanning is compatible with other point cloud data, such as LiDAR. This allows for merging data from different scanners to create a detailed 3D representation of a bridge, with varying point cloud densities for different components. This concept is shown below in Figure 26. Scanning data can also be used to generate finite element models for corrosion-damaged bridge components, helping to avoid inaccurate load postings. Future research includes generating finite-element input files from scanned geometry for estimating the capacity of corrosion-damaged elements and proposing a simplified design formulation for load ratings.

(a)

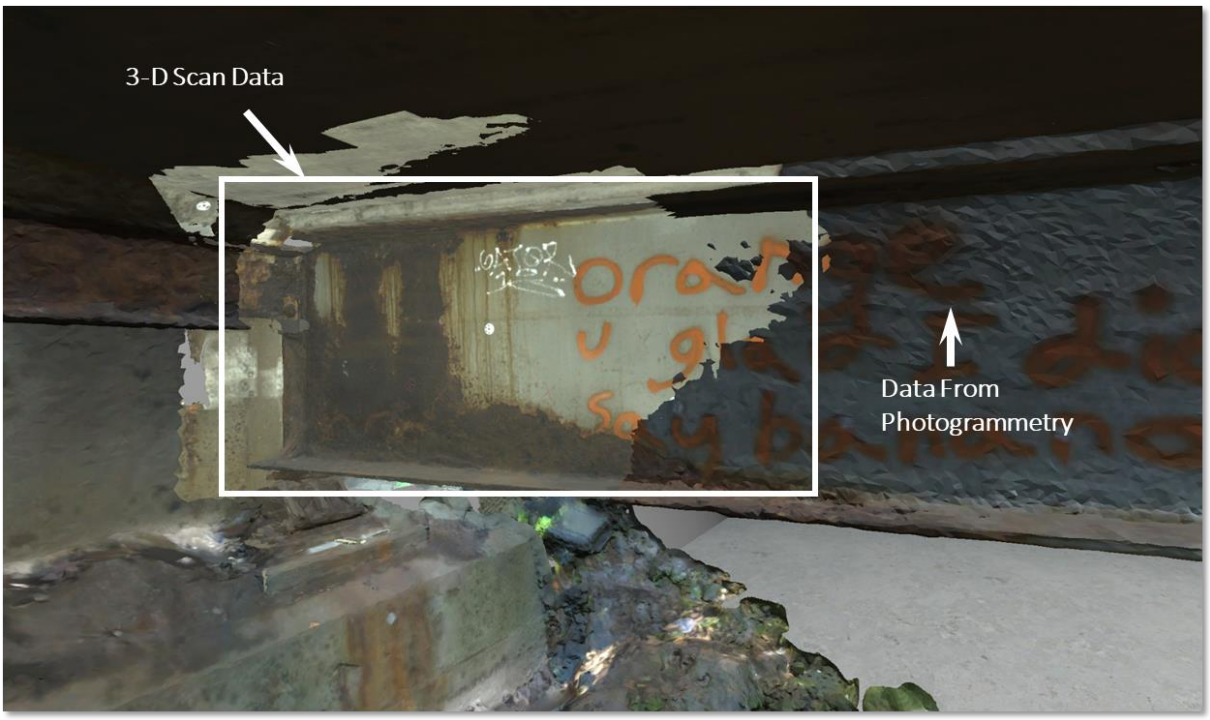

(b)

Figure 26. Representative image of combined 3D scanning and photogrammetry data sets showing a) zoomed-out view and b) zoomed-in view.

The results presented in this study are largely focused on the trials of the structured-light scanner. However, considering the potential cost savings and accessibility of photogrammetry as an alternative, additional research is needed to evaluate different cameras for this technique, with a particular emphasis on ease of use. A comprehensive comparison between various camera models and settings would provide valuable insights into their effectiveness in photogrammetry applications, potentially making the technology more accessible to a wider range of professionals in the field of bridge inspection and structural engineering.

The main motivation for expanding the scope of research to include photogrammetry is to take advantage of the cost savings and accessibility it offers compared to structured-light scanning. By conducting a thorough evaluation of photogrammetry cameras, future studies will contribute to a better understanding of the potential benefits and limitations of both structured-light scanning and photogrammetry in the context of bridge inspections and corrosion damage assessment. This will enable professionals to make informed decisions on the most suitable equipment and techniques for their needs, considering both the accuracy and cost-effectiveness of the available options.

5.2. Summary and Conclusions

In conclusion, this research project sought to explore the potential of handheld 3D scanning and photogrammetry for the section loss assessment of corroded steel beams in bridge inspections. The study involved laboratory evaluations, field trials, and data processing to assess the accuracy, ease of use, and applicability of these technologies in real-world scenarios. The results demonstrated that structured-light 3D scanning technology, such as the Artec Eva and Artec Leo scanners, can provide accurate measurements and detailed representations of corroded sections, offering

significant potential for improving the quality of bridge inspection data and simplifying the on-site data collection process. Photogrammetry, though not as extensively explored in this study, also showed promise as a cost-effective alternative for capturing accurate measurements and creating 3D models.

The findings from this study provide support for the use of 3D scanning as a tool for engineers to generate accurate inspection data on corroded regions of bridge beams. This data may be used to inform decisions regarding load postings, prioritization of rehabilitation projects, and the allocation of retrofit funds. Further research is needed to compare different camera models and settings for photogrammetry, as well as to explore the integration of 3D scanning data with other point cloud data, such as LiDAR, and its application in generating finite element models for corrosion-damaged bridge components. Overall, the research contributes valuable insights and highlights future research opportunities in the field of bridge inspection and structural engineering. Key findings are highlighted below:

- This proof-of-concept project explored the use of photogrammetry and 3D scanning for the inspection of steel bridge beams, aiming to reduce the subjective nature of visual inspections and provide a complete model of the structures. The method was compared with the handheld 3D laser scanning and structured-light scanning to evaluate its accuracy and efficiency in creating three-dimensional models.

- Structured-light scanning was found to produce accurate 3D models of beams with section loss from corrosion, which can supplement photographs and sketches used in inspection reports. Tracking deterioration over time through 3D scanning during biennial inspections offers an enhanced method for monitoring bridge components.

- The findings of this project indicate that photogrammetry is a comparable alternative to structured light scanning in generating accurate 3D beam models, although the data collection process can be more time-consuming. The camera evaluated posed challenges with maneuverability and lighting, making research into more compact devices, such as cell phones a promising alternative for space-constricted environments.

- However, the trial applications revealed that significant time and testing are required for both scanning and post-processing to achieve accurate and complete results for both hand held scanning and photogrammetry. As a result, conducting trial runs is highly recommended before attempting full inspections with a scanner.

- Combining detailed data from structured-light scanners with broader LiDAR scans offers the potential to create comprehensive 3D representations of bridges with select components modeled using higher-density point clouds. These full-bridge models can be valuable for engineers in various applications.
- Accurate 3D scan data enables engineers to make informed decisions regarding load postings, rehabilitation project prioritization, and retrofit fund allocation. Furthermore, the scan data can be used to construct finite element models for precise evaluations of the remaining load-carrying capacity of a beam.

Overall, this study highlights the potential benefits of incorporating advanced imaging technologies, such as photogrammetry and 3D scanning, into the inspection and maintenance of steel bridge infrastructure.

6. Implementation of Research Results

CTDOT anticipates adopting the scanning technology in the near future. With this implementation, there are short- and long-term goals. Short-term goals include using scan data to:

1. Perform quality assurance checks on inspections to verify section loss measurements.
2. Verify or obtain section loss measurements for load rating calculations.
3. Obtain section loss measurements for critical bridges, including those that face closure or load posting.

Long-term goals include:

1. Scanning corroded beam ends in subsequent inspection cycles and overlying the 3D models to determine the progression and rate of corrosion. The rate of corrosion may then be used for deterioration modeling.
2. Investigating 3D scanning for crack mapping. This application will require a proof-of-concept study prior to implementation.
3. Documenting bridge hits and using the model to monitor sections that don't require immediate repair and develop repairs for those that do.
4. Scanning for distortion caused by overloading or under designing members such as the web, gusset plates, etc.
5. Preserving and recreating historically significant details on bridges such as the ones located on the Merritt Parkway.
6. Developing criteria to determine when scan data should be used rather than conventional methods.
7. Creating visual aids for training designers and inspectors, as well as helping engineers and non-engineers understand field conditions.

References

1. Kayser JR, Nowak AS. Capacity loss due to corrosion in steel-girder bridges. Journal of Structural Engineering. 1989;115(6):1525-37.
2. Kulicki J, Prucz Z, Sorgenfrei D, Mertz D, Young W. Guidelines for evaluating corrosion effects in existing steel bridges. Washington, D.C.: Transportation Research Board; 1990.
3. Albhaisi S, Nassif H. Simple Approach to Calculate Displacements and Rotations in Integral Abutment Bridges. Transportation Research Record: Journal of the Transportation Research Board. 2015;2522:39-46.
4. National Bridge Inspection Standards. 23 CFR 650-3112004.
5. Agdas D, Rice JA, Martinez JR, Lasa IR. Comparison of visual inspection and structural-health monitoring as bridge condition assessment methods. Journal of Performance of Constructed Facilities. 2015;30(3):04015049.
6. Phares BM, Rolander DD, Graybeal BA, Washer GA. Reliability of visual bridge inspection. Public Roads. 2001;64(5).
7. Phares BM, Washer GA, Rolander DD, Graybeal BA, Moore M. Routine highway bridge inspection condition documentation accuracy and reliability. Journal of Bridge Engineering. 2004;9(4):403-13.
8. Fuchs P, Washer G, Chase S, Moore M. Applications of laser-based instrumentation for highway bridges. Journal of Bridge Engineering. 2004;9(6):541-9.
9. Jaselskis EJ, Gao Z, Walters RC. Improving transportation projects using laser scanning. Journal of Construction Engineering and Management. 2005;131(3):377-84.
10. Randall T. Construction engineering requirements for integrating laser scanning technology and building information modeling. Journal of Construction Engineering and Management. 2011;137(10):797-805.
11. Minehane M, O'Donovan R, Ruane K, O'Keeffe B, editors. The Use of 3D Laser Scanning Technology for Bridge Inspection and Assessment. Proceedings of Civil Engineering Research in Ireland (CERI) Conference 2016; August 28-29 2014; Belfast, Northern Ireland.
12. Ross RJ, Brashaw BK, Anderson SJ. Use of laser scanning technology to obtain as-built records of historic covered bridges. USDA Forest Service Report FPL-RP-6692012.
13. Yang H, Xu X, Neumann I. The benefit of 3D laser scanning technology in the generation and calibration of FEM models for health assessment of concrete structures. Sensors. 2014;14(11):21889-904.
14. Park H, Lee H, Adeli H, Lee I. A new approach for health monitoring of structures: terrestrial laser scanning. Computer-Aided Civil and Infrastructure Engineering. 2007;22(1):19-30.
15. Riveiro B, González-Jorge H, Varela M, Jáuregui DV. Validation of terrestrial laser scanning and photogrammetry techniques for the measurement of vertical underclearance and beam geometry in structural inspection of bridges. Measurement. 2013;46(1):784-94.
16. Olsen MJ, Kuester F, Chang BJ, Hutchinson TC. Terrestrial laser scanning-based structural damage assessment. Journal of Computing in Civil Engineering. 2009;24(3):264-72.
17. Artec3D. Professional 3D scanning solution. https://wwwartec3dcom/files/pdf/ArtecScanners-Booklet-EUROpdf2017.
18. McPherron SP, Gernat T, Hublin J-J. Structured light scanning for high-resolution documentation of in situ archaeological finds. Journal of Archaeological Science. 2009;36(1):19-24.

19. Hołowko E, Januszkiewicz K, Bolewicki P, Sitnik R, Michoński J. Application of multi-resolution 3D techniques in crime scene documentation with bloodstain pattern analysis. Forensic Science International. 2016;267:218-27.
20. Olesen OV, Paulsen RR, Hojgaard L, Roed B, Larsen R. Motion tracking for medical imaging: a nonvisible structured light tracking approach. IEEE Transactions on Medical Imaging. 2012;31(1):79-87.
21. Motley D. https://gomeasure3dcom/blog/how-structured-light-3d-scanners-work-video/ [Internet]: GoMeasure3D. Available from: https://gomeasure3d.com/blog/how-structured-light-3d-scanners-work-video/.
22. Hain A, Zaghi AE, Kamali A, Zaffetti RP, Overturf B, Pereira FE. Applicability of 3-D Scanning Technology for Section Loss Assessment in Corroded Steel Beams. Transportation Research Record. 2019:0361198119832887.
23. Artec3D. Artec Leo 2019 [Available from: https://www.artec3d.com/portable-3d-scanners/artec-leo.
24. Jiang R, Jáuregui DV, White KR. Close-range photogrammetry applications in bridge measurement: Literature review. Measurement. 2008;41(8):823-34.
25. Linder W. Digital photogrammetry: theory and applications: Springer Science & Business Media; 2013.
26. Hain A, Zaghi AE. Applicability of Photogrammetry for Inspection and Monitoring of Dry-Stone Masonry Retaining Walls. Transportation Research Record. 2020;2674(9):287-97.
27. Stavroulaki M, Riveiro B, Drosopoulos G, Solla M, Koutsianitis P, Stavroulakis GE. Modelling and strength evaluation of masonry bridges using terrestrial photogrammetry and finite elements. Advances in Engineering Software. 2016;101:136-48.
28. Joorabchian A, Peterman KD, editors. Using photogrammetry-based imperfection measurement tools to determine the impact of corner radii imperfection on cold-formed steel member strength. Proc of the Annual Stability Conference, Structural Stability Research Counsile; 2018.
29. Cavaco E, Pimenta R, Valença J. A new method for corrosion assessment of reinforcing bars based on close-range photogrammetry: Experimental validation. Structural Concrete. 2019;20(3):996-1009.
30. Sony α7R III 35 Mm Full-Frame Camera with Autofocus www.sony.com/electronics/interchangeable-lens-cameras/ilce-7rm3#product_details_default.: Sony Corporation of America; 2019 [
31. ZEISS Batis 2/25 Oberkochen, Germany: Carl Zeiss AG; 2019 [https://www.zeiss.com/camera-lenses/us/photography/products/batis-lenses/batis-225.html].
32. AD360II-C WITSTRO TTL Powerful & Portable Flash: GODOX Photo Equipment Co. Ltd; 2019 [http://www.godox.com/EN/Products_Camera_Flash_Witstro_AD360IIC_Powerfou&Portable_Flash.html].
33. Geng J. Structured-light 3D surface imaging: a tutorial. Advances in Optics and Photonics. 2011;3(2):128-60.
34. RealityCapture Bratislava, Slovakia: Capturing Reality s.r.o; 2019 [https://www.capturingreality.com/Product].

Appendixes

Appendix A – Video Tutorials for 3D Scanning for Corrosion Damage Assessment of Steel Beams

- Artec Leo 3D Scanner for Bridge Inspection Part 1- Scanner Basics: https://www.youtube.com/watch?v=2XPSoX6azj4&list=PLlEYKC2hlZDNlnjTMqmhZOGVc1DHj3X5C&index=1
- Artec Leo 3D Scanner for Bridge Inspection Part 2- Scanner Preparation and Usage: https://www.youtube.com/watch?v=nqPMZMiWAj8&list=PLlEYKC2hlZDNlnjTMqmhZOGVc1DHj3X5C&index=2
- Artec Leo 3D Scanner for Bridge Inspection Part 3- Processing in Artec Studio: https://www.youtube.com/watch?v=7BEp3WiYNqQ&list=PLlEYKC2hlZDNlnjTMqmhZOGVc1DHj3X5C&index=3
- Artec Leo 3D Scanner for Bridge Inspection Part 4- Manual Alignment: https://www.youtube.com/watch?v=oyalGdoDaJg&list=PLlEYKC2hlZDNlnjTMqmhZOGVc1DHj3X5C&index=4

Appendix B – Case Study on Photogrammetry for Dry Stone Masonry Retaining Wall Inspection

ABSTRACT

Dry-stone masonry retaining walls are vulnerable to bulging and leaning due to the lack of cohesion between stones. Currently, the structural integrity of these walls is mainly assessed by qualitative judgments informed by visual inspections. Photogrammetry has the potential to increase the quality and objectivity of retaining wall inspections. This technology uses a series of images to generate a detailed 3D model of a structure. Currently, this technology is most commonly used in civil engineering applications for mapping large areas, often using aerial photographs. In this study, photogrammetry is used in two field trials to evaluate its ability to create accurate, high-resolution 3D representations of masonry retaining walls in Connecticut. The 3D models were used to document the current in-situ conditions to provide a baseline for future comparisons, as well as show cross sections of vulnerable areas, such as bulges or tilts. In one trial, data was collected on two dates to show the progression of movement of the wall. This paper gives an overview of best practices for data collection and discusses results and observations from the field trials. The generated 3D models provide an enhanced form of inspection documentation including detailed representations of geometry and colors. It is expected that the material presented in this paper facilitates the adoption of this promising technology for the inspection of masonry retaining walls and other transportation infrastructure.

Keywords: Photogrammetry, Retaining Wall Inspection, Vulnerability Assessment, Point Cloud

INTRODUCTION

Dry-stone masonry retaining walls are structures built by interlocking stones without mortar (1). These walls were predominately built in the 19th and early 20th centuries and many remain in service today (2, 3). In fact, 25-35% of the retaining walls in National Park Service inventory are dry-stone gravity walls (4, 5). The main difference between dry-stone retaining walls and concrete walls or mortared masonry is the lack of cohesion between the stones due to the absence of concrete, grout, or mortar. While the rocks are arranged in an interlocking pattern, there are no mechanical connections between individual stones (6). This allows for internal deformation and sliding between the stacking planes (7). This makes the walls vulnerable to bulging and leaning, which in excess can lead to failure (8, 9). In addition to the vulnerabilities of this wall type, the design of such walls is often unclear. Until the 1960s and 1970s, the design of this wall type was poorly defined, with most construction based on a trial-and-error process (6). Currently, the structural integrity is primarily assessed by qualitative judgments informed by visual inspections (10). Visual inspections commonly include measurements such as total length, maximum height, and distance from the edge of the roadway. If notable bulges or tilts are noted, surveying tools may be used to record measurements at critical locations. The inadequacies of current assessment techniques, as well as a limited understanding of the behavior of such wall systems, leads to an increasing maintenance problem for highway authorities already challenged by limited funding.

Close-range photogrammetry has the potential to address the shortcomings in assessment techniques by enabling high-accuracy data collection along the entire wall length. The principle of photogrammetry is to calculate 3D coordinates from two or more photographs of the same object, taken at different orientations (11). Increasing the number of pictures increases the number of reference points, which results in a greater likelihood of correctly calculating the coordinates. The 3D model can then be generated using a reference scale included in the pictures, and measurements can be extracted. Close-range photogrammetry describes applications in which the imaging distance is less than 300 m (984 ft) (12). The concept of using photogrammetry for capturing measurements on transportation infrastructure has been reported since the 1980's (13). However, its use has increased due to advancements in camera resolution that have led to accuracies of 0.1 mm -10 mm (0.004 in- 0.4 in) for objects between 0.5 m and 200 m (1.6 ft - 656 ft)(14). Photogrammetry is commonly used in the civil engineering field by state Departments of Transportation for large-scale mapping of transportation systems, construction sites, and topographical mapping, often using aerial images (15-17). Recently, photogrammetry has been used on smaller scale structures to obtain geometric measurements on bridges (18-20), capture movements of retaining walls in a series of experiments (7, 21), and obtain estimates for the displacement of a retaining wall following an earthquake (22).

The geometric information collected using photogrammetry can be represented as a point cloud or surface mesh and can capture the color and texture of an object. This data may be used to generate 3D renderings for as-builts and to supplement photographs in inspection reports. In addition to obtaining accurate geometric information over the length of the structure, this technology offers several other advantages for use in monitoring and inspecting retaining walls including: 1) evaluating failure progression by overlaying 3D models generated from data collected at different times, 2) enabling the user to capture cross-sectional images of the wall to view bulges, and 3)

providing a baseline 3D model to compare other types of inspection data. Such features make photogrammetry attractive for the inspection and monitoring of retaining walls, and for incorporation into asset management systems. Asset management requires a 1) comprehensive inventory, 2) condition assessment of the inventory, and 3) data to make predictions and plan for future needs (23). While LiDAR has been noted for asset management of retaining walls (24), photogrammetry also warrants consideration as it is applicable to all aspects of the asset management workflow including documentation, inspection, and rate of change analysis.

To evaluate the potential of this technology for masonry retaining walls, a feasibility study was conducted by researchers at the University of Connecticut (UCONN) in partnership with the Connecticut Department of Transportation (CTDOT). The study consisted of two field trials of retaining walls in Connecticut. The suitability of the technology for inspection was based on the ability to capture the geometry, color, and texture along the full length of the retaining wall, as well as detailed information on local areas vulnerable to failure, such as those bulging or tilting. The potential for monitoring was evaluated by collecting data from one of the sites on different dates to compare the progression of local deformations over time. Data from both field trials were used to generate 3D models, which were able to represent the detail of the individual stones as well as the overall geometry of the walls. Section cuts were taken in the 3D models to demonstrate the severity of tilting or bulging in the wall. Using photogrammetry has the potential to improve the quality of the inspection and monitoring program of masonry retaining walls by providing geometric information at every point on the wall, rather than a select set of points taken with a total station.

This paper provides an overview of the theory of photogrammetry, the equipment, and software required for data collection and data processing, as well as results, general observations, and conclusions from two field trials of this image-based monitoring method. It is anticipated that the conclusions and observations presented will provide support for the use of photogrammetry as a tool for engineers to monitor masonry retaining walls and other transportation infrastructure. This data may be used to inform decisions regarding the prioritization of repair projects and the allocation of funds.

Overview of photogrammetry

Theory

Photogrammetry uses methods of image measurement and interpretation to derive the three-dimensional coordinates of an object from multiple images of that body. In principle, photogrammetry can be applied in any situation where the user can capture images of an object. When taking pictures, a three-dimensional object is reduced to a two-dimensional image, which corresponds to a loss of information. Areas of the object that are not visible in the image cannot be reconstructed. This includes full sections that are not captured, as well as regions with a lack of contrast or components too small to be recognized by the camera. This concept is critical to keep in mind when capturing images for use in photogrammetry and will be discussed in the Data Collection section of this paper.

Once the images are collected, methods of image interpretation and measurement are required that identify points in images by geometric and radiometric data (i.e. intensity, color value, grey

value). Similar points between images are identified, and mathematical transformations between image and object space are employed from these measurements, resulting in a 3D model of the object (14).

Equipment

To evaluate the applicability of using photogrammetry for the inspection of retaining walls, it was first necessary to find commercially available equipment to capture pictures and a computer with a powerful graphics processing unit (GPU) to process the data. While a standalone GPU is not required for photogrammetry, it substantially increases the speed of processing. A powerful GPU is required by the software that was chosen in this study. The most critical pieces of equipment are the camera and lens used to capture images. Photogrammetry relies on the ability to detect features in an image. Higher-resolution cameras allow the sensor to resolve small features from further distances. For this reason, the Sony a7RIII with a 42-megapixel 35-mm full-frame sensor was selected (25). The lens chosen was the low-distortion Zeiss Batis 2/25 with a focal length of 25 mm, an aperture range of f/2 to f/22, and a minimum focusing range of 0.2 m (8 in) (26). This wide-angle lens has a large field of view, which decreases the number of images required while providing the large overlap between images that is needed for future image processing. Using a low-distortion lens limits the distortion compensation required in data processing and significantly improves the quality of raw data. Distortion happens when the image scale is not constant throughout the entire image field and causes straight lines to bend inward or outwards from the center of the image. In addition to the camera and lens, a powerful flash was needed to provide even lighting and mitigate slight variations in natural light. To alleviate the differences in lighting onsite, a Godox flash (27) was used. The camera, lens, and flash are shown in Figure 6. a.

In this study, a desktop computer was used to run the software that processed the images and generated the 3D model (AMD Ryzen Threadripper 2990WX CPU at 3.0 GHz, 128 GB RAM, and ZOTAC GeForce GTX 1080 Ti 22GB GDDR5X GPU). This computer was chosen to increase the processing speed. The software, RealityCapture, was used to generate the 3D model and will be discussed in the data processing section of the paper.

Data Collection

The accuracy, quality, and completeness of the 3D model generated from photogrammetry is dependent on serval factors. This section will review suggestions for coverage of a scene, as well as the reference objects required during data collection.

Coverage

Photogrammetry works by identifying common objects in a series of photographs. This requires overlap between images, pictures taken from different orientations, and complete coverage of the object to generate a comprehensive 3D model. For large structures such as retaining walls, it is critical to capture images from a distance to provide a baseline reference scene, as well as close-range pictures to increase the accuracy of the model. Through data-collection trials, it was found that the distance between passes should be less than two times the distance of the previous pass. Similarly, an overlap of images is important within a given pass. This overlap in both directions allows for tie points to be automatically selected by the software or added manually. The distance of the

first pass should be based on the desired level of detail of the model and the resolution of the camera. This can be informed through trials and/or calculations based on sensor size, focal length, and resolution.

For the software to generate depth maps and the 3D coordinate system, images of the object are needed from different perspectives. This requires multiple images of each section of wall at different horizonal and vertical orientations. This can be accomplished by taking steps to the left or right and standing or crouching to collect images from every angle. Both the number of passes, as well as the number images with different orientations, should be increased for areas of concern that require additional detail.

The most important aspect of image collection is complete coverage of all areas of interest. To ensure this, an image collection plan should be made prior to arriving on site. The plan should note the distance of each pass, the distance between the images within a pass to provide adequate overlap, the range of camera heights during each pass (which is dependent on the geometry of the wall), and areas on the wall that require higher resolution, such as bulges. Data collection should be methodical. Additional coordination and communication are required when more than one person is collecting images to ensure complete coverage.

Reference Objects

Photogrammetry requires user input to correctly represent the scale of a scene. This can be accomplished by measuring an object within the scene and using it as a reference, such as the length of the wall, or by including scale markers. For high-accuracy applications, using scale markers is preferred, as they provide known measurements rather than estimations. Scale markers should be easy to identify within images, contain references with known dimensions, and be placed on a rigid backing to prevent distortion of the scale marker. In this trial, two types of markers, grid and cross-type, were printed and affixed to thick glass or fiberglass backings. The markers are shown in Figure 6. b. In the software, these markers are used to define distance relationships.

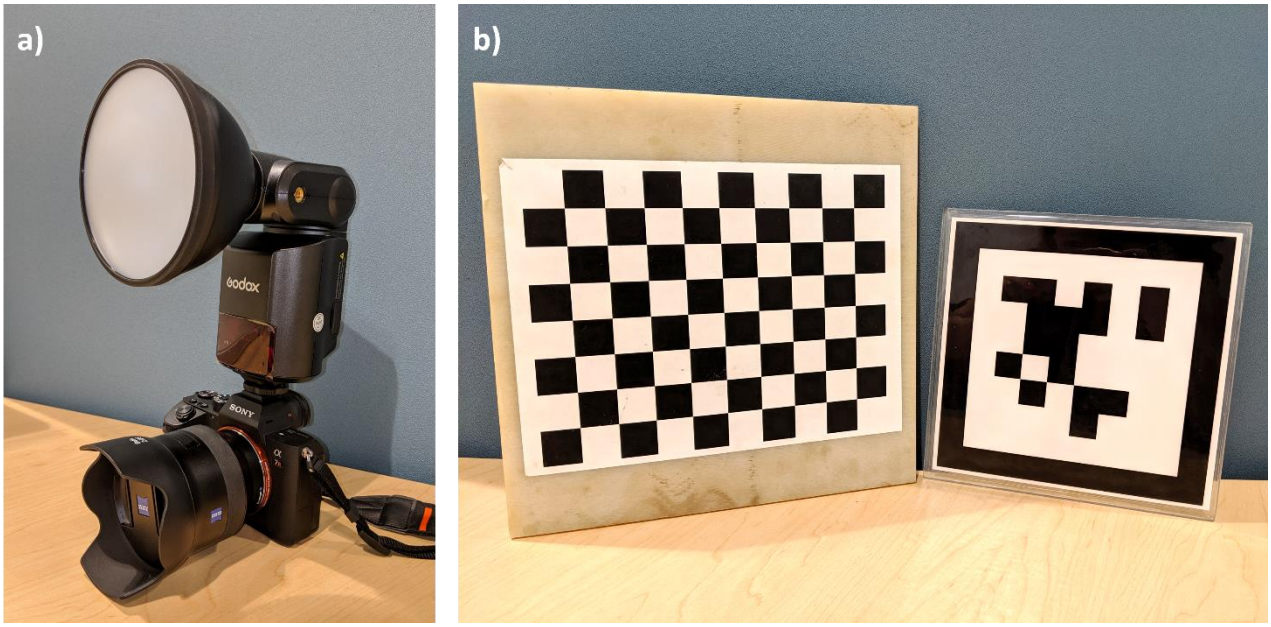

Figure 1. Equipment used for photogrammetry including the a) camera, lens and flash and b) reference markers.

Data Processing

All processing of the images takes place offsite. Prior to processing, all images that are not relevant, not correctly exposed, or out of focus should be removed from the batch. After the initial sorting is complete, the images are imported to RealityCapture in JPG format. RealityCapture is a commercially available, all-in-one photogrammetry software that automatically extracts 3D models from images (28). This software is unique in its speed, ability to produce high-polygon meshes, and built-in editing and mesh simplification features.

The first step in processing is defining the camera calibration. This involves inputting the camera parameters including the 35-mm equivalent focal length, sensor size, principal point, and the aspect ratio. The lens distortion parameters are calculated in the software for individual images using the Brown polynomial model for radial distortion (29). After importing and calibrating, the images need to be aligned. This is done by first performing a draft alignment and then adding control points to the image. Control points can be either tie-points or ground control points. Ground control points are those with a known x, y, and z, and can be defined using traditional survey measurements, existing plans, or lidar. Tie points are distinct features that are visible in multiple images from different viewpoints. Points are autogenerated but can also be manually added to help link images or components together that the software is having difficulty joining automatically. As this was a trial setting to determine applicability of the workflow and focused on local regions, no ground control points were included. For future applications, ground control points should be added to reduce error accumulations, particularly over models with larger areas.

The points are also used to add reference measurements to the scene. Once the distance constraints are applied, the model is updated and realigned. An alignment report for the model is generated that notes the projection error, which is the difference in pixel position between a point in a photo and the projection of the corresponding 3D point in the same photo. Ideally, the median error should be around 0.5 pixels, and not above 1 pixel. If the error is above this threshold, additional control points are added. These should be manually added to the model by selecting common features in multiple images and should be included at locations where there are not already control points. The alignment process is then run again. This process is repeated until the target accuracy is achieved. A longer measurement, relative to the alignment markers, can also be used as a check for the generated model.

After alignment, the final step in processing is to generate a mesh. This is the most time-consuming operation and the speed is dependent upon the complexity of the model, resolution and number of images used, and the processing power of the computer. To decrease the processing time, non-critical areas can be left out of the defined “Reconstruction Region”. The final mesh can then be used for measurements or be exported to other software to obtain additional information or visualizations.

To evaluate the potential of close-range photogrammetry for masonry retaining walls, a feasibility study was conducted on two retaining walls in Connecticut. The phases varied based on purpose of the trial as well as size and location of the walls.

Field Evaluation 1

The first feasibility study was a two-part field trial of using photogrammetry on a masonry retaining wall in Connecticut (**Error! Reference source not found.**a). The wall was selected by CTDOT and had a total length of approximately 45 m (150 ft) and a maximum height of approximately 4.5 m (15 ft). The wall had a significant bulge (**Error! Reference source not found.**b), and CTDOT was concerned the bulge was worsening, particularly after heavy rainfall events. Therefore, the research team collected baseline data, and returned to the site one week later following a rainfall of approximately 36 mm (1.4 in).

Each onsite data collection consisted of approximately 850 images collected over the course of 1 hour. Eight of the crosshair reference scales were used. The references were distributed along the length of the wall. The same coverage plan was used for both data collections and consisted of three passes at various distances. The first pass was approximately 1 m (3.3 ft) from the wall, at the edge of the shoulder. This offset distance was chosen to ensure the generated model would have a dense point cloud, particularly at the bulge area, to be able to detect relative movements between the models from the two data collections. The goal was to capture movements of as small as 1 mm (.04 in). This offset distance was also optimal for the flash to highlight the shadowed areas between the stones. The second pass was at approximately 3 m (9.8 ft) and the third was on the opposite side of the two-lane road, approximately 9 m (29.5 ft) from the wall. Traffic control was required to close the lane closest to the wall for the first and second passes. Additional images were captured at the bulge region at a closer distance. This series of images was taken approximately 0.5 m (1.6 ft) from the wall. Taking images at closer distances results in a denser point cloud, which increases the resolution of the model at this location.

The data from each date was processed to generate two 3D models. The purpose of this trial was to determine if photogrammetry could be used to collect accurate 3D information on a masonry retaining wall and if the models generated from the two dates could be compared to show potential movement of the wall. To monitor the movement, fixed points that are not on the walls should be included to allow for comparison of the point clouds collected at different times. For this trial, storm drains on the shoulder and a concrete block at the base of a telephone pole were used as fixed points. Depending on the duration of monitoring, fixed points must be chosen or added to the site accordingly.

The initial processed models had average point densities of approximately 3,100,000 points/m^2 (288,000 points/ft^2); but they were simplified for additional processing to an average of 31,000 points/m^2 (2,880 points/ft^2).The final models of the field scans represented an area of approximately 150 m^2 (1,615 ft^2) and consisted of more than 4 million vertices (**Error! Reference source not found.**c and **Error! Reference source not found.**d). The final 3D meshes were each approximately 1 GB in size with texture resolutions of 16384x16384 pixel.

Figure 2. Retaining wall from Field Trial 1 in Connecticut showing a) overall view of wall, b) closeup of bulge region, c) image of 3D model of wall, and d) point cloud.

Field Evaluation 2

The second feasibility study used photogrammetry as a post-event inspection technique. The wall was selected by CTDOT and had a total length of approximately 90 m (295 ft) and a maximum height of approximately 9 m (30 ft). This larger wall was chosen to show the feasibility of using the technology to collect information on large areas, while maintaining the level of detail. In one location, the wall had a significant bulge, and in another location, there was a severe tilt (**Error! Reference source not found.**a). The retaining wall supported a two-lane road above. A fire hydrant next to the roadway broke, causing a surplus of water to drain behind the wall. As such, the department wanted to collect baseline information to determine the current condition of the site and the stability and safety of the roadway. This field trial involved inspection on one date.

Data collection consisted of approximately 1,250 images collected over the course of two hours. A 25-ft extendable tripod was used to take pictures on the higher regions of the wall. The camera was remotely triggered using the Bluetooth capabilities of the camera and a Sony cell phone application. Drones may provide a viable option to reduce the time required for data collection on structures of

a similar scale. However, even without a drone, data was able to be collected on the upper portions of the wall, and the time required onsite was not a deterrent.

Four crosshair scales, two grid scales, and a 4.9-m (16-ft) surveying scale were used as reference measurements. The surveying scale was not used to scale the model but was used as a check to ensure the scaling using the markers was accurate over a larger distance. The location made image collection challenging, as a building ran along the length of the wall with variable offset distances. This, combined with the long length of the wall, made collecting overall images impossible. Three passes were used where space allowed, and two passes were used in the other locations. The first, second, and third passes were approximately 1 m (3.3 ft), 3 m (9.8 ft), and 6 m (20 ft) from the wall, respectively. Additional images were captured at the bulge and tilted regions.

The data was processed to generate a 3D model. The purpose of this trial was to determine if the access constraints and size of the wall would affect the quality of the 3D model, as well to provide valuable information to the department on the current state of the wall. The initial processed model had an average point density of 1,940,000 points/m^2 (180,200 points/ft^2); but it was simplified for additional processing to an average of 54,000 points/m^2 (5,040 points/ft^2). The final model of the field scan represented an area of approximately 600 m^2 (6,500 ft^2) and consisted of nearly 30 million vertices (**Error! Reference source not found.**b). The relative accuracy of the model was obtained by comparing measurements in the model to known measurements such as those from the tape measure or surveying rod. Fifteen linear measurements were compared ranging from 0.305 m (1ft) to 3.96 m (13 ft). Measurements were only compared for distances that were not defined using tie points. The RMS error was 0.15% with the largest magnitude of error being -0.26% and the smallest magnitude being 0.066%. The final 3D mesh was approximately 5 GB in size with a texture resolution of 16384x16384 pixel.

Figure 3. Retaining wall from Field Trial 2 in Connecticut showing a) picture from site and b) snip of 3D model.

RESULTS

Field Evaluation 1

The success of the field evaluation was based on the quality of the 3D representation of the wall, the ability to overlay the models from both dates to see changes in the overall geometry, and the ease of use of the technology onsite. For the first criterion, quality was based on the completeness of the 3D model. An overall view of the model was shown in **Error! Reference source not found.**c. Additional close up views of the model show the overall mesh in the bulge region (**Error! Reference source not found.**a) and the point cloud (**Error! Reference source not found.**b). The fidelity of the photogrammetry is demonstrated by the realistic nature of the 3D model. The surface roughness of the rocks and variations in colors and sizes of the stones contributed to the successful data processing, as there were many distinct features the software could recognize.

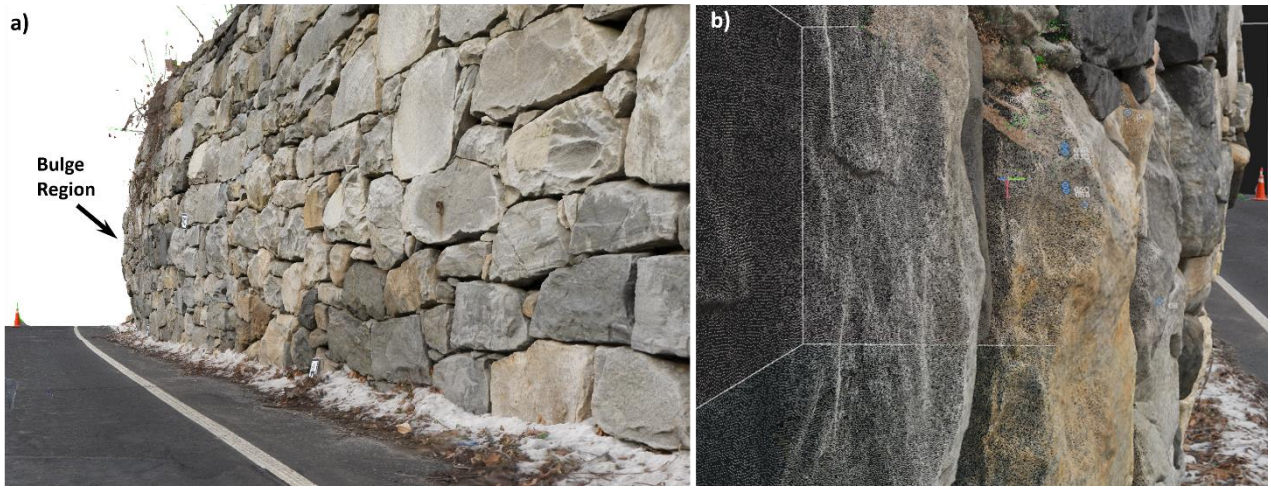

Figure 4. Views of 3D model generated with photogrammetry for Field Trial 1 including a) overall view of bulge region and b) example of high-density point cloud.

In addition to viewing the photogrammetry data in RealityCapture, supplementary software, such as Blender (30), can be used to provide further clarity on the in-situ geometry of a structure. Blender allows for viewing 3D variations in geometry or between models in 2D using color maps. Common comparisons include the deviation from a flat plane as well as differences between data sets collected at different times. This software provides one additional option for making the results easier to visualize. In this trial, it was used to show the difference in geometry between the two 3D models generated from data collected on different dates. The models were overlaid, and color mapping was used to show the movement of the wall (Figure 5). The average maximum displacement of the wall was between 4 mm - 6 mm (0.16 in – 0.24 in). Due to the surface roughness of the wall, an average maximum displacement is reported rather than an absolute maximum. This data showed that the entire wall was moving outwards, not just the bulge region. This triggered the department to take precautionary measures to prevent rubble from falling into the roadway, should a full or partial portion of the wall fail.

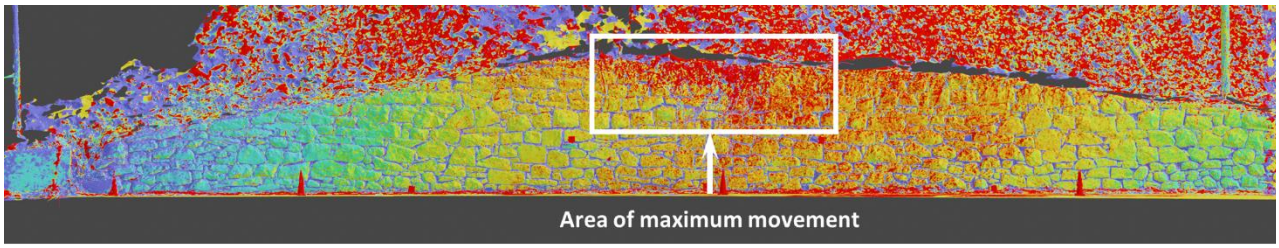

Figure 5. Color map showing movement of retaining wall between the two 3D models.

The feasibility of using the technology onsite was determined per discussions with CTDOT personnel present during data collection. It was noted that one lane of the road needed to be closed for traditional inspections of the wall due to the limited shoulder, and as such, this requirement for photogrammetry was not additionally restrictive. The consensus was that the hour of data collection in the field was reasonable and the quality of the data justified the time required onsite.

Field Evaluation 2

Field Trial 2 aimed to provide visualizations to show the current condition of the wall. One visualization created was the model of the entire structure. The comprehensive detail of the 3D model was previously shown in **Error! Reference source not found.**. In addition, other software can be used to highlight critical regions of the wall. Both color mapping and section cuts were used to show the geometry of the local areas of concern. These added visuals put the model in context and show the user where to focus within the comprehensive model.

Blender was used to create a color map to highlight the severity of the bulge (**Error! Reference source not found.**a). This figure shows the deviation from a reference plane that was defined based on the geometry of other portions of the wall. This type of visualization provides significant insight into the condition of the structure and extent of the bulge area and reveals details that are not immediately evident in the typical illustrations and pictures currently used in inspections. This type of image can also be helpful to show the progression of bulging over time, by keeping the color scale the same, and monitoring how the colors progress.

Another method to show the extent of the bulge region is using section cuts, as shown in **Error! Reference source not found.**b. The section cuts were taken in Artec Studio (31), a software used for data processing of 3D scans. While this software is commonly used for capturing and processing data from Artec scanners, it accepts a variety of file types for input and easily works for models with up to 500 million polygons. It was selected as the section cuts tool is easy to work with and had been used in other projects for generating similar visualizations. The section cut tool can be used at any location along the wall to define horizontal or vertical planes. This tool can be used to identify areas of maximum movement. This tool is also beneficial for finding individual stones within the wall that are displacing faster than others in the immediate vicinity. The section cut method can also be used to show the severity of leaning occurring on the opposite end of the wall (**Error! Reference source not found.**c). While masonry walls allow for large deformations prior to failure, the extent that is allowable is largely unknown. Tracking the tilt progression of walls over time using section cuts could lead to a better understanding of the deformation capacity of such structures.

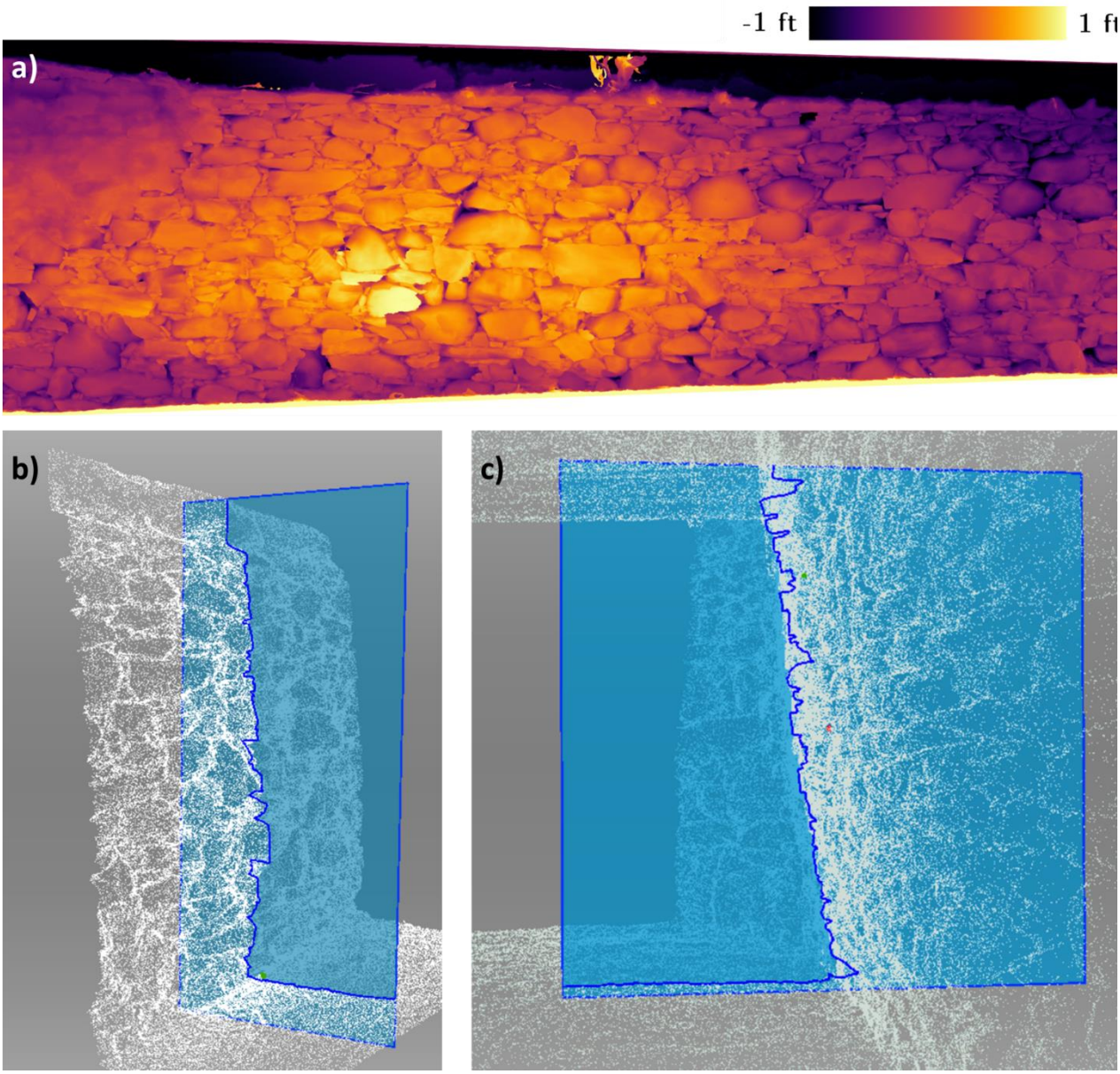

Figure 6. Supplemental visualizations for Field Trial 2 including a) color map to show size and extent of bulge region and section cuts to show b) bulge region and c) extent of tilt.

DISCUSSION

The results of the field trial using photogrammetry for inspection and monitoring of retaining walls were promising. It is important to keep in mind the scope of this study, and not to draw conclusions for other applications until similar trials are conducted. The distinctive nature of masonry retaining walls in terms of the surface texture, size, and color of the stones make them a perfect application for photogrammetry, as the individual features of the wall can be easily recognized in software and matched in corresponding images. For structures with less surface detail, such as reinforced concrete retaining walls, the software may have difficulty finding commonalities in images and thus issues when generating the 3D model. Further trials are needed to investigate this.

When using the technology on masonry retaining walls, the goals of the application should be clear prior to data collection. For example, when performing monitoring of a local area prone to failure, data collection of the full wall may not be required. Capturing data on smaller areas reduces complexity in both data collection and data processing. This may also allow for higher accuracy models by reducing the distances of the passes and capturing more images. While the same method can be used to increase the accuracy of larger objects, this method can be tedious and time-consuming, due to the number of images and processing time required.

For continued monitoring, permanent markers should be noted at or added to the site. These markers should be guaranteed to stay in place for the duration of monitoring and are needed to compare models generated from different dates. For example, using storm drains that are near the object of concern is one option, but it should be noted that the position could change with activities such as road paving. Markers such as trees or telephone poles should not be used as they are subject to slight movements. In addition, the user should consider the time of year when conducting the inspection. In spring, summer, and fall, plant growth can obscure areas of the wall or markers, thus limiting the amount of data collected.

This technology also has significant potential to be combined with unmanned aerial vehicles (UAVs). While using photogrammetry with UAVs is common, the difference between current methods and the approach discussed in this paper is the equipment used and the corresponding level of detail. However, due to the increased payload capacity of drones, the current equipment can simply be used in a modified setup. This approach offers significant potential, as the flight path of drones can be programmed to ensure comprehensive coverage during image collection.

The main advantage of this technology is its ability to provide a 3-D model with accurate geometric data at each point on a site, whereas traditional surveying methods only provide detailed information at a select set of points. While the current capabilities of this technology are impressive, cost-effectiveness and accuracy are only anticipated to improve. The software and imaging sectors are making vast improvements in the quality of their products and the presence of many competitors is driving prices down. Photogrammetry has the potential to improve the inspection of many types of transportation infrastructure. Low equipment costs (<$7,500) and the number of potential applications may make the initial investment in both money and time to learn the technology worthwhile for state DOTs and consulting firms. As 3D models become mainstream in the future, photogrammetry is likely to emerge as a frontrunner for generating models that represent current site conditions. However, future research should consider a comparison of photogrammetry to laser scanning in accuracy, time required in the field and in post-processing, and cost for different monitoring applications. This comparison would provide a baseline to evaluate the absolute accuracy of the photogrammetry method as opposed to the relative accuracy. It is anticipated that this information will help researchers and practitioners decide what method is best suited to their needs, capabilities, and constraints.

CONCLUSIONS

A proof-of-concept study was conducted using photogrammetry for the inspection and monitoring of two masonry retaining walls in Connecticut. Using photogrammetry provides a comprehensive 3D model of the entire wall, which can be used to provide detailed inspection data and provide a

baseline for future comparison. This technology helps remove the subjectivity associated with visual inspections. The resulting data sets from the trials were detailed digital replications of the originals, which provided a model where measurements and section cuts could be extracted and analyzed. The results of the two-phase trial showed that the application of photogrammetry for the inspection of retaining walls is feasible and the results are promising. Significant findings from this trial are outlined below:

- Photogrammetry can be used to produce accurate 3D models of masonry retaining walls. Such models can be used to identify local areas subject to failure and can supplement the information in inspection reports.
- Using photogrammetry in subsequent inspections would provide an enhanced method to track movement over time. This can be used to monitor changes at local areas or along the full length of the wall.
- Accurate 3D models of in-situ conditions enable engineers to make informed decisions regarding the need for repair, replacement, or increased monitoring of structures. Having comprehensive, objective data can help with the prioritization of projects and allocation of funds.
- Combining this technology with UAVs provides an opportunity to eliminate the personnel time required on-site and to optimize data collection through programming of flight paths.

ACKNOWLEDGEMENTS

The support of Leo Fontaine, Michael McDonnell, Aron Steeves, Scott Bushee, Sara Ghatee, Robert Pion, and Mathew Calkins in setting up the field trials is also recognized. The contribution of Timothy Henning in processing the data is acknowledged.

REFERENCES

1. Colas A, Morel J, Garnier D. Yield design of dry-stone masonry retaining structures—Comparisons with analytical, numerical, and experimental data. International journal for numerical and analytical methods in geomechanics. 2008;32(14):1817-32.
2. O'Reilly M, Bush D, Brady K, Powrie W, editors. The stability of drystone retaining walls on highways. Proceedings of the Institution of Civil Engineers: Municipal Engineer; 1999.
3. Oetomo JJ, Vincens E, Dedecker F, Morel JC. Modeling the 2D behavior of dry-stone retaining walls by a fully discrete element method. International Journal for Numerical and Analytical Methods in Geomechanics. 2016;40(7):1099-120.
4. DeMarco MJ, Anderson SA, Armstrong A. Retaining Walls Are Assets Too! *Public roads*. 2009;73(1).
5. Anderson SA, DeMarco MJ, Keough D, Lewis S. Preliminary Results from the National Park Service Retaining Wall Inventory Program. *Proceedings of the 59th Highway Geology Symposium*; Sante Fe, New Mexico; May, 2008. p. 72-90.

6. Mack DA, Sanders SH, Millhone WL, Fippin RL, Kennedy DG. *Rockery Design and Construction Guidelines*. Publication No. FHWA-CFL/TD-06-006. US Federal Highway Administration Central Federal Lands Highway Division; 2006.
7. Villemus B, Morel J, Boutin C. Experimental assessment of dry stone retaining wall stability on a rigid foundation. *Engineering structures*. 2007;29(9):2124-32.
8. Walker P, McCombie P, Claxton M. Plane strain numerical model for drystone retaining walls. *Proceedings of the Institution of Civil Engineers-Geotechnical Engineering*. 2007;160(2):97-103.
9. Eschenasy D. Condition Assessment of Old Stone Retaining Walls. *STRUCTURE magazine*; 2015.
10. Claxton M, Hart RA, McCombie PF, Walker PJ. Rigid block distinct-element modeling of dry-stone retaining walls in plane strain. *Journal of geotechnical and geoenvironmental engineering*. 2005;131(3):381-9.
11. Linder W. *Digital photogrammetry: theory and applications.* Springer Science & Business Media; 2013.
12. Wolf PR, Dewitt BA. *Elements of photogrammetry: with applications in GIS*. McGraw-Hill New York; 2000.
13. Bales FB. Close-range photogrammetry for bridge measurement. *Transportation Research Record: Journal of the Transportation Research Board*, 1985. 950:39-44.
14. Luhmann T, Robson S, Kyle S, Boehm J. *Close-range photogrammetry and 3D imaging*. Walter de Gruyter; 2013.
15. *Photogrammetrics.* Minnesota Department of Transportation, Photogrammetric Unit. Available at: https://www.dot.state.mn.us/surveying/photogrammetrics.html. Accessed March 25, 2020.
16. S*pecifications for Photogrammetric Stereocompilation.* New York State Department of Transportation, Photogrammetry Section Technical Resource Center; 2005. Available at: https://www.dot.ny.gov/divisions/engineering/design/design-services/photogrammetry/repository/2005spec.pdf. Accessed March 25, 2020.
17. Krot E. *PennDOT uses Photogrammetry to Measure Up*. PennDOT Way; August 27, 2018. Available at: https://www.penndot.gov/PennDOTWay/Pages/Article.aspx?post=151
18. Riveiro B, González-Jorge H, Varela M, Jáuregui DV. Validation of terrestrial laser scanning and photogrammetry techniques for the measurement of vertical underclearance and beam geometry in structural inspection of bridges. *Measurement*. 2013;46(1):784-94.
19. Jáuregui DV, Tian Y, Jiang R. Photogrammetry Applications in Routine Bridge Inspection and Historic Bridge Documentation. *Transportation Research Record: Journal of the Transportation Research Board.* 2006;1958(1):24-32.
20. Jáuregui DV, White KR, Woodward CB, Leitch KR. Noncontact photogrammetric measurement of vertical bridge deflection. *Journal of Bridge Engineering*. 2003;8(4):212-22.
21. Oats RC, Escobar-Wolf R, Oommen T. A Novel Application of Photogrammetry for Retaining Wall Assessment. *Infrastructures*. 2017;2(3):10.
22. Ko Y-Y, Han J-Y, Chou J-Y. Application of close-range photogrammetry for post-failure reconnaissance of a retaining wall. *Geotechnical Hazards from Large Earthquakes and Heavy Rainfalls.* Springer; 2017. p. 503-12.

23. Anderson SA, Alzamora D, DeMarco MJ. Asset Management Systems for Retaining Walls. *Geo-Velopment: The Role of Geological and Geotechnical Engineering in New and Redevelopment Projects.* 2009. p. 162-77.
24. *Transportation Research Synthesis: Asset Management for Retaining Walls.* Prepared by C.C Associates. Minnesota Department of Transportation; 2013. Available at: https://lrrb.org/media/reports/TRS1305.pdf.
25. *Sony α7R III 35 Mm Full-Frame Camera with Autofocus*. Sony Corporation of America; 2019. Avaiolable at: https://www.sony.com//electronics//interchangeable-lens-cameras//ilce-7rm3#product_details_default. Accessed July 15, 2019.
26. *ZEISS Batis 2/25.* Carl Zeiss, Inc. Available at: https://www.zeiss.com/consumer-products/us/photography/batis/batis-225.html. Accessed July 15, 2019.
27. *AD360II-C WITSTRO TTL Powerful & Portable Flash*. GODOX Photo Equipment Co. Ltd. Available at: http://www.godox.com/EN/Products_Camera_Flash_Witstro_AD360IIC_Powerfou&Portable_Flash.html. Accessed July 15, 2019.
28. *RealityCapture.* Capturing Reality s.r.o. Available at:https://www.capturingreality.com/Product. Accessed July 15, 2020.
29. Brown DC. Decentering distortion of lenses. *Photogrammetric Engineering and Remote Sensing*. 1966.
30. *About.* blender; Available at: https://www.blender.org/about/. Accessed March 25, 2020.
31. *Artec Studio 14*. Artec3D. Available at: https://www.artec3d.com/3d-software/artec-studio. Accessed on March 25, 2020.